Supplementary Materials:

Pivalate complexes of copper(II) with aliphatic amines as potential precursors for depositing nanomaterials from the gas phase

A. Butrymowicz-Kubiak, W. Luba, K. Madajska, T. Muzioł, I. B. Szymańska*
Faculty of Chemistry, Nicolaus Copernicus University in Toruń, Gagarina 7, 87-100 Toruń, Poland

X-ray crystal structure determination

Table S1 Crystal data and structure refinement for **(1a−4a)**.

Identification code	(1a)	(2a)	(3a)	(4a)
Empirical formula	C38 H76 Cu3 N2 O12	C38 H76 Cu3 N2 O12	C26 H56 Cu3 N2 O10	C82 H207 Cu20 N7 O72
Formula weight	943.62	943.62	747.34	3732.48
Temperature [K]	100(2) K	100(2) K	100(2) K	100(2) K
Wavelength [Å]	1.54184 Å	1.54184 Å	1.54184 Å	1.54184 Å
Crystal system, space group	Monoclinic, $P2_1/n$	Monoclinic, $P2_1/n$	Triclinic, $P\bar{1}$	Orthorhombic, Pbca
Unit cell dimensions [Å] and [°]	a = 11.6627(5) Å α= 90° b = 12.4671(6) Å β= 92.366(4)° c = 16.7859(9) Å γ = 90°	a = 12.5325(5) Å α= 90° b = 11.1446(4) Å β= 94.728(4)° c = 17.1279(7) Å γ = 90°	a = 6.2514(12) Å α= 109.72(2)° b = 12.462(4) Å β= 99.887(15)° c = 12.7926(14) Å γ = 103.83(2)°	a = 20.1618(5) Å α= 90° b = 25.4106(6) Å β= 90° c = 28.8931(7) Å γ = 90°
Volume [Å^3]	2438.6(2) Å^3	2384.10(17) Å^3	875.5(4) Å^3	14802.6(6) Å^3
Z, Calculated density [Mg×m^{-3}]	2, 1.285 Mg/m^3	2, 1.314 Mg/m^3	1, 1.417 Mg/m^3	4, 1.675 Mg/m^3
Absorption coefficient [mm^{-1}]	1.958 mm^{-1}	2.002 mm^{-1}	2.532 mm^{-1}	3.784 mm^{-1}
F(000)	1002	1002	393	7688
Crystal size [mm]	0.160 x 0.100 x 0.040 mm^3	0.130 x 0.060 x 0.040 mm^3	0.100 x 0.030 x 0.020 mm^3	0.080 x 0.050 x 0.030 mm^3
Theta range for data collection [°]	2.635 to 74.499°	4.739 to 68.227°	3.819 to 68.199°	3.189 to 74.501°
Limiting indices	-13<=h<=14, -15<=k<=15, -20<=l<=20	-15<=h<=15, -13<=k<=13, -20<=l<=20	-7<=h<=6, -13<=k<=13, -20<=l<=20	-12<=h<=25, -31<=k<=31, -34<=l<=35
Reflections collected/unique	18846	6871	6231	59548
Completeness [%] to theta [°]	99.9 %	98.0 %	88.7 %	99.7 %
Absorption correction	Gaussian	Analytical	Gaussian	Gaussian
Max. and min. transmission	1.000 and 0.618	0.921 and 0.798	1.000 and 0.806	0.932 and 0.816
Refinement method	Full-matrix least-squares on F^2	Full-matrix least-squares on F^2	Full-matrix least-squares on F^2	Full-matrix least-squares on F^2
Data/restraints/parameters	4859 / 42 / 333	6871 / 32 / 276	2831 / 29 / 199	14603 / 51 / 898
Goodness-of-fit on F^2	1.025	1.034	1.032	1.045
Final R Indices [I>2sigma(I)]	R1 = 0.0478, wR2 = 0.1244	R1 = 0.0716, wR2 = 0.1940	R1 = 0.1094, wR2 = 0.2815	R1 = 0.0432, wR2 = 0.1240
R indices (all data)	R1 = 0.0528, wR2 = 0.1275	R1 = 0.0934, wR2 = 0.2117	R1 = 0.1846, wR2 = 0.3288	R1 = 0.0486, wR2 = 0.1277
Largest diff. peak and hole [eÅ^{-3}]	0.684 and -0.790 e.Å^{-3}	1.036 and -0.601 e.Å^{-3}	1.919 and -1.063 e.Å^{-3}	1.635 and -0.898 e.Å^{-3}

Table S2 Bond lengths [Å] and angles [°] for $[Cu_3(^tBuNH_2)_2(\mu\text{-}O_2C^tBu)_6]_n$ **(1a)**.

Cu(1)-O(1)	1.947(2)
Cu(1)-O(2)#1	1.954(2)
Cu(1)-O(12)#1	1.973(2)
Cu(1)-O(11)	1.977(2)
Cu(1)-O(22)	2.136(2)
Cu(1)-Cu(1)#1	2.6022(8)
Cu(2)-O(21)	1.964(2)
Cu(2)-O(21)#2	1.964(2)
Cu(2)-N(31)#2	1.994(3)
Cu(2)-N(31)	1.994(3)
O(1)-Cu(1)-O(2)#1	169.07(9)
O(1)-Cu(1)-O(12)#1	90.79(10)
O(2)#1-Cu(1)-O(12)#1	88.89(10)
O(1)-Cu(1)-O(11)	89.67(10)
O(2)#1-Cu(1)-O(11)	88.54(10)
O(12)#1-Cu(1)-O(11)	168.77(9)
O(1)-Cu(1)-O(22)	93.74(10)
O(2)#1-Cu(1)-O(22)	97.00(10)
O(12)#1-Cu(1)-O(22)	102.40(8)
O(11)-Cu(1)-O(22)	88.76(8)
O(21)-Cu(2)-O(21)#2	180.0
O(21)-Cu(2)-N(31)#2	84.95(10)
O(21)#2-Cu(2)-N(31)#2	95.05(10)
O(21)-Cu(2)-N(31)	95.05(10)
O(21)#2-Cu(2)-N(31)	84.95(10)
N(31)#2-Cu(2)-N(31)	180.00(14)

Symmetry transformations used to generate equivalent atoms:
#1 -x+1,-y+1,-z+1 #2 -x+2,-y+1,-z+1

Table S3 Bonds lengths [Å] and angles [°] for $[Cu_3(^sBuNH_2)_2(\mu\text{-}O_2C^tBu)_6]_n$ **(2a)**.

Cu(1)-O(12)#1	1.940(4)
Cu(1)-O(11)	1.952(4)
Cu(1)-O(2)#1	1.974(3)
Cu(1)-O(1)	1.978(4)
Cu(1)-O(21)	2.160(3)
Cu(1)-Cu(1)#1	2.6277(13)
Cu(2)-O(22)	1.962(4)
Cu(2)-O(22)#2	1.962(4)
Cu(2)-N(31)	2.023(6)
Cu(2)-N(31)#2	2.023(6)
O(12)#1-Cu(1)-O(11)	168.46(16)
O(12)#1-Cu(1)-O(2)#1	90.93(19)
O(11)-Cu(1)-O(2)#1	89.03(18)
O(12)#1-Cu(1)-O(1)	89.3(2)
O(11)-Cu(1)-O(1)	88.40(19)
O(2)#1-Cu(1)-O(1)	168.12(15)
O(12)#1-Cu(1)-O(21)	95.69(16)
O(11)-Cu(1)-O(21)	95.61(16)
O(2)#1-Cu(1)-O(21)	101.92(14)
O(1)-Cu(1)-O(21)	89.88(14)
O(12)#1-Cu(1)-Cu(1)#1	82.74(12)
O(11)-Cu(1)-Cu(1)#1	85.86(12)
O(2)#1-Cu(1)-Cu(1)#1	81.07(10)
O(1)-Cu(1)-Cu(1)#1	87.18(11)
O(21)-Cu(1)-Cu(1)#1	176.67(10)
O(22)-Cu(2)-O(22)#2	180.0
O(22)-Cu(2)-N(31)	92.3(2)
O(22)#2-Cu(2)-N(31)	87.7(2)
O(22)-Cu(2)-N(31)#2	87.7(2)
O(22)#2-Cu(2)-N(31)#2	92.3(2)
N(31)-Cu(2)-N(31)#2	180.0
C(2)-O(1)-Cu(1)	119.6(3)
C(2)-O(2)-Cu(1)#1	127.2(3)
C(12)-O(11)-Cu(1)	121.1(4)
C(12)-O(12)-Cu(1)#1	125.1(4)
C(22)-O(21)-Cu(1)	148.8(3)

C(22)-O(22)-Cu(2)	111.2(3)
C(32)-N(31)-Cu(2)	120.0(6)
Cu(2)-N(31)-H(31A)	107.3
Cu(2)-N(31)-H(31B)	107.3
Cu(2)-N(31)-H(31C)	107.3
Cu(2)-N(31)-H(31D)	107.3

Symmetry transformations used to generate equivalent atoms:

#1 -x+1,-y+1,-z+1 #2 -x+1,-y+2,-z+1

Table S4 Bonds lengths [Å] and angles [°] for $[Cu_3(^iPrNH_2)_2(\mu_3\text{-}OH)_2(\mu\text{-}O_2C^tBu)_4]_n$ **(3a)**.

Cu(1)-O(31)#1	1.951(6)
Cu(1)-O(31)	1.951(6)
Cu(1)-O(11)#1	1.975(8)
Cu(1)-O(11)	1.975(7)
Cu(2)-O(31)	1.936(7)
Cu(2)-O(1)	1.950(9)
Cu(2)-N(21)	1.990(8)
Cu(2)-O(12)#1	2.083(9)
Cu(2)-O(31)#2	2.127(7)
O(31)#1-Cu(1)-O(31)	180.0(5)
O(31)#1-Cu(1)-O(11)#1	83.6(3)
O(31)-Cu(1)-O(11)#1	96.4(3)
O(31)#1-Cu(1)-O(11)	96.4(3)
O(31)-Cu(1)-O(11)	83.6(3)
O(11)#1-Cu(1)-O(11)	180.0
O(31)-Cu(2)-O(1)	93.0(3)
O(31)-Cu(2)-N(21)	171.3(4)
O(1)-Cu(2)-N(21)	94.1(4)
O(31)-Cu(2)-O(12)#1	92.8(3)
O(1)-Cu(2)-O(12)#1	140.0(3)
N(21)-Cu(2)-O(12)#1	85.1(4)
O(31)-Cu(2)-O(31)#2	81.6(3)
O(1)-Cu(2)-O(31)#2	135.1(3)
N(21)-Cu(2)-O(31)#2	89.8(3)
O(12)#1-Cu(2)-O(31)#2	84.8(3)
C(2)-O(1)-Cu(2)	115.6(8)
Cu(2)-O(31)-Cu(1)	112.9(4)
Cu(2)-O(31)-Cu(2)#2	98.4(3)
Cu(1)-O(31)-Cu(2)#2	131.1(4)
Cu(2)-O(31)-H(31)	103.9
Cu(1)-O(31)-H(31)	103.9
Cu(2)#2-O(31)-H(31)	103.9

Symmetry transformations used to generate equivalent atoms:

#1 -x+1,-y+1,-z+1 #2 -x+2,-y+1,-z+1

Table S5 Bond lengths [Å] and angles [°] for $[Cu_{20}(EtNH_2)_6(\mu_3\text{-}OH)_{24}(OH)(H_2O)_5(NO_3)(\mu\text{-}O_2C^tBu)_8](^tBuCO_2)_6\cdot 13H_2O$ **(4a)**.

Cu(1)-O(1)	1.924(3)
Cu(1)-N(81)	1.976(3)
Cu(1)-O(105)	1.986(2)
Cu(1)-O(110)	2.026(2)
Cu(1)-O(101)	2.274(2)
Cu(1)-Cu(9)	2.9024(7)
Cu(1)-Cu(2)	2.9926(7)
Cu(2)-O(102)	1.942(2)
Cu(2)-O(101)	1.944(2)
Cu(2)-O(106)	1.967(2)
Cu(2)-O(105)	1.982(2)
Cu(2)-Cu(3)	3.0575(7)
Cu(3)-O(11)	1.935(2)
Cu(3)-N(76)	1.983(3)
Cu(3)-O(107)	1.984(2)
Cu(3)-O(106)	2.010(2)
Cu(3)-O(102)	2.258(2)
Cu(3)-Cu(10)	2.9937(7)
Cu(3)-Cu(4)	3.0279(7)
Cu(4)-O(102)	1.950(2)
Cu(4)-O(108)	1.959(3)
Cu(4)-O(103)	2.008(2)
Cu(4)-O(107)	2.016(2)
Cu(4)-O(90)	2.374(4)
Cu(4)-O(12)	2.414(2)
Cu(4)-O(88)	2.428(4)
Cu(5)-N(91)	1.987(4)
Cu(5)-O(103)	1.998(2)
Cu(5)-O(85)	2.025(3)
Cu(5)-O(109)	2.044(3)
Cu(5)-O(86)	2.289(4)
Cu(5)-O(108)	2.325(3)
Cu(5)-Cu(6)	2.9733(7)
Cu(6)-O(104)	1.932(2)
Cu(6)-O(109)	1.962(2)

Cu(6)-O(103)	1.978(2)
Cu(6)-O(112)#1	1.995(2)
Cu(6)-Cu(7)	3.0012(7)
Cu(7)-O(21)	1.923(3)
Cu(7)-O(31)	1.930(3)
Cu(7)-O(111)	1.984(2)
Cu(7)-O(112)#1	2.026(2)
Cu(7)-O(104)	2.245(2)
Cu(7)-Cu(8)	2.9532(7)
Cu(7)-Cu(10)#1	2.9568(7)
Cu(8)-O(101)	1.933(2)
Cu(8)-O(104)	1.939(2)
Cu(8)-O(110)	1.976(2)
Cu(8)-O(111)	1.978(2)
Cu(8)-O(32)	2.274(2)
Cu(9)-O(108)#1	1.932(3)
Cu(9)-O(105)	1.939(2)
Cu(9)-O(110)	1.970(2)
Cu(9)-O(109)#1	1.982(2)
Cu(9)-O(90)#1	2.228(4)
Cu(10)-O(111)#1	1.955(2)
Cu(10)-O(107)	1.957(2)
Cu(10)-O(106)	1.961(2)
Cu(10)-O(112)	1.964(2)
Cu(10)-O(88)	2.209(4)
Cu(10)-O(89)	2.308(5)
O(1)-Cu(1)-N(81)	94.63(12)
O(1)-Cu(1)-O(105)	93.49(11)
N(81)-Cu(1)-O(105)	170.65(11)
O(1)-Cu(1)-O(110)	166.22(11)
N(81)-Cu(1)-O(110)	92.03(11)
O(105)-Cu(1)-O(110)	79.07(9)
O(1)-Cu(1)-O(101)	114.95(11)
N(81)-Cu(1)-O(101)	102.83(11)
O(105)-Cu(1)-O(101)	77.80(8)
O(110)-Cu(1)-O(101)	75.09(8)
O(1)-Cu(1)-Cu(9)	125.49(9)
N(81)-Cu(1)-Cu(9)	129.02(9)

O(105)-Cu(1)-Cu(9)	41.68(7)
O(110)-Cu(1)-Cu(9)	42.66(6)
O(101)-Cu(1)-Cu(9)	88.39(6)
O(1)-Cu(1)-Cu(2)	95.49(8)
N(81)-Cu(1)-Cu(2)	142.22(9)
O(105)-Cu(1)-Cu(2)	40.99(6)
O(110)-Cu(1)-Cu(2)	86.52(6)
O(101)-Cu(1)-Cu(2)	40.51(6)
Cu(9)-Cu(1)-Cu(2)	70.552(17)
O(102)-Cu(2)-O(101)	94.50(9)
O(102)-Cu(2)-O(106)	85.29(9)
O(101)-Cu(2)-O(106)	175.63(9)
O(102)-Cu(2)-O(105)	173.98(10)
O(101)-Cu(2)-O(105)	86.27(9)
O(106)-Cu(2)-O(105)	94.39(9)
O(102)-Cu(2)-Cu(1)	141.73(7)
O(101)-Cu(2)-Cu(1)	49.44(7)
O(106)-Cu(2)-Cu(1)	129.56(7)
O(105)-Cu(2)-Cu(1)	41.10(6)
O(102)-Cu(2)-Cu(3)	47.50(7)
O(101)-Cu(2)-Cu(3)	138.04(7)
O(106)-Cu(2)-Cu(3)	40.27(7)
O(105)-Cu(2)-Cu(3)	133.55(7)
Cu(1)-Cu(2)-Cu(3)	153.15(2)
O(11)-Cu(3)-N(76)	91.26(13)
O(11)-Cu(3)-O(107)	96.50(10)
N(76)-Cu(3)-O(107)	167.95(13)
O(11)-Cu(3)-O(106)	175.55(10)
N(76)-Cu(3)-O(106)	93.11(12)
O(107)-Cu(3)-O(106)	79.05(9)
O(11)-Cu(3)-O(102)	102.75(10)
N(76)-Cu(3)-O(102)	109.95(12)
O(107)-Cu(3)-O(102)	77.35(9)
O(106)-Cu(3)-O(102)	76.47(9)
O(11)-Cu(3)-Cu(10)	135.18(8)
N(76)-Cu(3)-Cu(10)	129.64(11)
O(107)-Cu(3)-Cu(10)	40.23(7)
O(106)-Cu(3)-Cu(10)	40.47(6)

O(102)-Cu(3)-Cu(10)	81.80(6)
O(11)-Cu(3)-Cu(4)	88.84(8)
N(76)-Cu(3)-Cu(4)	148.68(11)
O(107)-Cu(3)-Cu(4)	41.20(7)
O(106)-Cu(3)-Cu(4)	87.83(6)
O(102)-Cu(3)-Cu(4)	40.08(6)
Cu(10)-Cu(3)-Cu(4)	65.981(16)
O(11)-Cu(3)-Cu(2)	141.03(8)
N(76)-Cu(3)-Cu(2)	94.96(10)
O(107)-Cu(3)-Cu(2)	84.79(7)
O(106)-Cu(3)-Cu(2)	39.24(6)
O(102)-Cu(3)-Cu(2)	39.36(6)
Cu(10)-Cu(3)-Cu(2)	62.880(15)
Cu(4)-Cu(3)-Cu(2)	66.714(16)
O(102)-Cu(4)-O(108)	177.58(11)
O(102)-Cu(4)-O(103)	98.42(9)
O(108)-Cu(4)-O(103)	83.25(10)
O(102)-Cu(4)-O(107)	84.18(9)
O(108)-Cu(4)-O(107)	94.21(10)
O(103)-Cu(4)-O(107)	176.80(10)
O(102)-Cu(4)-O(90)	102.84(13)
O(108)-Cu(4)-O(90)	75.66(13)
O(103)-Cu(4)-O(90)	80.40(12)
O(107)-Cu(4)-O(90)	100.89(12)
O(102)-Cu(4)-O(12)	91.79(9)
O(108)-Cu(4)-O(12)	89.81(10)
O(103)-Cu(4)-O(12)	94.85(9)
O(107)-Cu(4)-O(12)	83.17(9)
O(90)-Cu(4)-O(12)	165.10(12)
O(102)-Cu(4)-O(88)	77.86(12)
O(108)-Cu(4)-O(88)	100.02(13)
O(103)-Cu(4)-O(88)	106.15(12)
O(107)-Cu(4)-O(88)	76.17(12)
O(12)-Cu(4)-O(88)	157.65(12)
O(102)-Cu(4)-Cu(3)	48.19(7)
O(108)-Cu(4)-Cu(3)	130.91(8)
O(103)-Cu(4)-Cu(3)	141.13(7)
O(107)-Cu(4)-Cu(3)	40.41(7)

O(90)-Cu(4)-Cu(3)	121.15(11)
O(12)-Cu(4)-Cu(3)	71.00(6)
O(88)-Cu(4)-Cu(3)	87.57(10)
N(91)-Cu(5)-O(103)	171.17(15)
N(91)-Cu(5)-O(85)	94.03(16)
O(103)-Cu(5)-O(85)	91.82(11)
N(91)-Cu(5)-O(109)	94.82(15)
O(103)-Cu(5)-O(109)	79.18(9)
O(85)-Cu(5)-O(109)	170.97(11)
N(91)-Cu(5)-O(86)	85.19(18)
O(103)-Cu(5)-O(86)	101.40(13)
O(85)-Cu(5)-O(86)	90.40(16)
O(109)-Cu(5)-O(86)	92.10(14)
N(91)-Cu(5)-O(108)	97.60(15)
O(103)-Cu(5)-O(108)	74.69(9)
O(85)-Cu(5)-O(108)	101.80(11)
O(109)-Cu(5)-O(108)	75.26(9)
O(86)-Cu(5)-O(108)	167.22(14)
N(91)-Cu(5)-Cu(6)	134.56(13)
O(103)-Cu(5)-Cu(6)	41.36(7)
O(85)-Cu(5)-Cu(6)	130.62(10)
O(109)-Cu(5)-Cu(6)	41.02(7)
O(86)-Cu(5)-Cu(6)	86.39(10)
O(108)-Cu(5)-Cu(6)	82.77(7)
O(104)-Cu(6)-O(109)	175.49(10)
O(104)-Cu(6)-O(103)	93.87(10)
O(109)-Cu(6)-O(103)	81.69(10)
O(104)-Cu(6)-O(112)#1	87.07(10)
O(109)-Cu(6)-O(112)#1	97.39(10)
O(103)-Cu(6)-O(112)#1	178.37(10)
O(104)-Cu(6)-Cu(5)	132.86(7)
O(109)-Cu(6)-Cu(5)	43.16(7)
O(103)-Cu(6)-Cu(5)	41.87(7)
O(112)#1-Cu(6)-Cu(5)	136.80(7)
O(104)-Cu(6)-Cu(7)	48.40(7)
O(109)-Cu(6)-Cu(7)	136.04(8)
O(103)-Cu(6)-Cu(7)	138.28(7)
O(112)#1-Cu(6)-Cu(7)	42.11(7)

Cu(5)-Cu(6)-Cu(7)	152.75(2)
O(21)-Cu(7)-O(31)	89.04(12)
O(21)-Cu(7)-O(111)	175.83(11)
O(31)-Cu(7)-O(111)	93.30(10)
O(21)-Cu(7)-O(112)#1	98.19(11)
O(31)-Cu(7)-O(112)#1	168.22(12)
O(111)-Cu(7)-O(112)#1	78.95(9)
O(21)-Cu(7)-O(104)	106.09(10)
O(31)-Cu(7)-O(104)	108.60(10)
O(111)-Cu(7)-O(104)	76.43(9)
O(112)#1-Cu(7)-O(104)	78.43(9)
O(21)-Cu(7)-Cu(8)	142.00(8)
O(31)-Cu(7)-Cu(8)	87.09(8)
O(111)-Cu(7)-Cu(8)	41.72(6)
O(112)#1-Cu(7)-Cu(8)	92.79(7)
O(104)-Cu(7)-Cu(8)	41.03(6)
O(21)-Cu(7)-Cu(10)#1	135.28(9)
O(31)-Cu(7)-Cu(10)#1	128.13(9)
O(111)-Cu(7)-Cu(10)#1	40.98(6)
O(112)#1-Cu(7)-Cu(10)#1	41.38(7)
O(104)-Cu(7)-Cu(10)#1	86.44(6)
Cu(8)-Cu(7)-Cu(10)#1	72.434(17)
O(21)-Cu(7)-Cu(6)	93.99(8)
O(31)-Cu(7)-Cu(6)	147.87(9)
O(111)-Cu(7)-Cu(6)	85.88(7)
O(112)#1-Cu(7)-Cu(6)	41.33(7)
O(104)-Cu(7)-Cu(6)	40.06(6)
Cu(8)-Cu(7)-Cu(6)	71.062(17)
Cu(10)#1-Cu(7)-Cu(6)	68.152(16)
O(101)-Cu(8)-O(104)	96.68(9)
O(101)-Cu(8)-O(110)	84.47(9)
O(104)-Cu(8)-O(110)	170.67(9)
O(101)-Cu(8)-O(111)	171.84(9)
O(104)-Cu(8)-O(111)	84.13(9)
O(110)-Cu(8)-O(111)	93.43(9)
O(101)-Cu(8)-O(32)	99.48(9)
O(104)-Cu(8)-O(32)	96.61(9)
O(110)-Cu(8)-O(32)	92.32(9)

O(111)-Cu(8)-O(32)	88.47(9)
O(101)-Cu(8)-Cu(7)	142.49(7)
O(104)-Cu(8)-Cu(7)	49.48(7)
O(110)-Cu(8)-Cu(7)	131.74(7)
O(111)-Cu(8)-Cu(7)	41.89(6)
O(32)-Cu(8)-Cu(7)	73.41(6)
O(108)#1-Cu(9)-O(105)	172.57(11)
O(108)#1-Cu(9)-O(110)	95.34(10)
O(105)-Cu(9)-O(110)	81.61(9)
O(108)#1-Cu(9)-O(109)#1	86.30(11)
O(105)-Cu(9)-O(109)#1	94.99(10)
O(110)-Cu(9)-O(109)#1	165.67(10)
O(108)#1-Cu(9)-O(90)#1	79.80(13)
O(105)-Cu(9)-O(90)#1	107.56(13)
O(110)-Cu(9)-O(90)#1	107.19(13)
O(109)#1-Cu(9)-O(90)#1	87.12(13)
O(108)#1-Cu(9)-Cu(1)	131.25(8)
O(105)-Cu(9)-Cu(1)	42.95(7)
O(110)-Cu(9)-Cu(1)	44.20(7)
O(109)#1-Cu(9)-Cu(1)	126.16(7)
O(90)#1-Cu(9)-Cu(1)	130.07(11)
O(111)#1-Cu(10)-O(107)	95.08(10)
O(111)#1-Cu(10)-O(106)	168.79(9)
O(107)-Cu(10)-O(106)	80.89(9)
O(111)#1-Cu(10)-O(112)	81.17(9)
O(107)-Cu(10)-O(112)	165.02(10)
O(106)-Cu(10)-O(112)	100.02(10)
O(111)#1-Cu(10)-O(88)	102.65(13)
O(107)-Cu(10)-O(88)	82.76(13)
O(106)-Cu(10)-O(88)	87.29(13)
O(112)-Cu(10)-O(88)	112.20(14)
O(111)#1-Cu(10)-O(89)	99.84(14)
O(107)-Cu(10)-O(89)	113.74(14)
O(106)-Cu(10)-O(89)	91.35(14)
O(112)-Cu(10)-O(89)	81.22(14)
O(111)#1-Cu(10)-Cu(7)#1	41.73(7)
O(107)-Cu(10)-Cu(7)#1	127.58(7)
O(106)-Cu(10)-Cu(7)#1	134.62(7)

O(112)-Cu(10)-Cu(7)#1	42.99(7)
O(88)-Cu(10)-Cu(7)#1	126.25(11)
O(111)#1-Cu(10)-Cu(3)	131.29(7)
O(107)-Cu(10)-Cu(3)	40.91(7)
O(106)-Cu(10)-Cu(3)	41.69(7)
O(112)-Cu(10)-Cu(3)	134.64(7)
O(88)-Cu(10)-Cu(3)	92.59(11)
O(89)-Cu(10)-Cu(3)	115.10(13)
Cu(7)#1-Cu(10)-Cu(3)	140.41(2)
C(2)-O(1)-Cu(1)	121.3(2)
C(12)-O(11)-Cu(3)	126.5(2)
C(12)-O(12)-Cu(4)	127.1(2)
C(22)-O(21)-Cu(7)	123.4(2)
C(32)-O(31)-Cu(7)	125.8(2)
C(32)-O(32)-Cu(8)	126.7(2)
C(79)-N(76)-Cu(3)	125.0(5)
C(77)-N(76)-Cu(3)	118.3(4)
Cu(3)-N(76)-H(76B)	107.7
Cu(3)-N(76)-H(76C)	106.1
Cu(3)-N(76)-H(76D)	106.1
C(82)-N(81)-Cu(1)	119.6(2)
Cu(1)-N(81)-H(81A)	107.4
Cu(1)-N(81)-H(81B)	107.4
C(92)-N(91)-Cu(5)	107.3(6)
C(94)-N(91)-Cu(5)	122.1(7)
Cu(5)-N(91)-H(91A)	110.3
Cu(5)-N(91)-H(91B)	110.3
Cu(5)-N(91)-H(91C)	106.8
Cu(5)-N(91)-H(91D)	106.8
N(87)-O(88)-Cu(10)	123.7(3)
N(87)-O(88)-Cu(4)	130.3(3)
Cu(10)-O(88)-Cu(4)	89.85(15)
N(87)-O(89)-Cu(10)	120.2(3)
N(87)-O(90)-Cu(9)#1	124.1(3)
N(87)-O(90)-Cu(4)	132.1(3)
Cu(9)#1-O(90)-Cu(4)	90.24(15)
Cu(5)-O(85)-H(85A)	117.8
Cu(5)-O(85)-H(85B)	125.0

Cu(5)-O(86)-H(86A)	113.3
Cu(5)-O(86)-H(86B)	136.5
Cu(8)-O(101)-Cu(2)	117.71(11)
Cu(8)-O(101)-Cu(1)	94.55(9)
Cu(2)-O(101)-Cu(1)	90.05(8)
Cu(8)-O(101)-H(101)	116.4
Cu(2)-O(101)-H(101)	116.4
Cu(1)-O(101)-H(101)	116.4
Cu(2)-O(102)-Cu(4)	118.56(12)
Cu(2)-O(102)-Cu(3)	93.14(9)
Cu(4)-O(102)-Cu(3)	91.73(9)
Cu(2)-O(102)-H(102)	116.0
Cu(4)-O(102)-H(102)	116.0
Cu(3)-O(102)-H(102)	116.0
Cu(6)-O(103)-Cu(5)	96.77(10)
Cu(6)-O(103)-Cu(4)	113.43(11)
Cu(5)-O(103)-Cu(4)	102.14(10)
Cu(6)-O(103)-H(103)	114.2
Cu(5)-O(103)-H(103)	114.2
Cu(4)-O(103)-H(103)	114.2
Cu(6)-O(104)-Cu(8)	126.74(12)
Cu(6)-O(104)-Cu(7)	91.54(9)
Cu(8)-O(104)-Cu(7)	89.49(9)
Cu(6)-O(104)-H(104)	113.9
Cu(8)-O(104)-H(104)	113.9
Cu(7)-O(104)-H(104)	113.9
Cu(9)-O(105)-Cu(2)	120.59(12)
Cu(9)-O(105)-Cu(1)	95.37(10)
Cu(2)-O(105)-Cu(1)	97.91(10)
Cu(9)-O(105)-H(105)	113.4
Cu(2)-O(105)-H(105)	113.4
Cu(1)-O(105)-H(105)	113.4
Cu(10)-O(106)-Cu(2)	106.95(10)
Cu(10)-O(106)-Cu(3)	97.84(10)
Cu(2)-O(106)-Cu(3)	100.49(10)
Cu(10)-O(106)-H(106)	116.3
Cu(2)-O(106)-H(106)	116.3
Cu(3)-O(106)-H(106)	116.3

Cu(10)-O(107)-Cu(3)	98.86(10)
Cu(10)-O(107)-Cu(4)	111.23(11)
Cu(3)-O(107)-Cu(4)	98.39(10)
Cu(10)-O(107)-H(107)	115.3
Cu(3)-O(107)-H(107)	115.3
Cu(4)-O(107)-H(107)	115.3
Cu(9)#1-O(108)-Cu(4)	113.98(14)
Cu(9)#1-O(108)-Cu(5)	93.89(10)
Cu(4)-O(108)-Cu(5)	92.98(10)
Cu(9)#1-O(108)-H(108)	117.1
Cu(4)-O(108)-H(108)	117.1
Cu(5)-O(108)-H(108)	117.1
Cu(6)-O(109)-Cu(9)#1	106.55(11)
Cu(6)-O(109)-Cu(5)	95.82(10)
Cu(9)#1-O(109)-Cu(5)	101.69(11)
Cu(6)-O(109)-H(109)	116.6
Cu(9)#1-O(109)-H(109)	116.6
Cu(5)-O(109)-H(109)	116.6
Cu(9)-O(110)-Cu(8)	118.16(11)
Cu(9)-O(110)-Cu(1)	93.14(9)
Cu(8)-O(110)-Cu(1)	101.49(10)
Cu(9)-O(110)-H(110)	113.8
Cu(8)-O(110)-H(110)	113.8
Cu(1)-O(110)-H(110)	113.8
Cu(10)#1-O(111)-Cu(8)	125.24(11)
Cu(10)#1-O(111)-Cu(7)	97.29(10)
Cu(8)-O(111)-Cu(7)	96.40(10)
Cu(10)#1-O(111)-H(111)	111.6
Cu(8)-O(111)-H(111)	111.6
Cu(7)-O(111)-H(111)	111.6
Cu(10)-O(112)-Cu(6)#1	114.97(12)
Cu(10)-O(112)-Cu(7)#1	95.63(10)
Cu(6)#1-O(112)-Cu(7)#1	96.56(10)
Cu(10)-O(112)-H(112)	115.5
Cu(6)#1-O(112)-H(112)	115.5
Cu(7)#1-O(112)-H(112)	115.5

Symmetry transformations used to generate equivalent atoms:

#1 -x+1,-y+1,-z+1

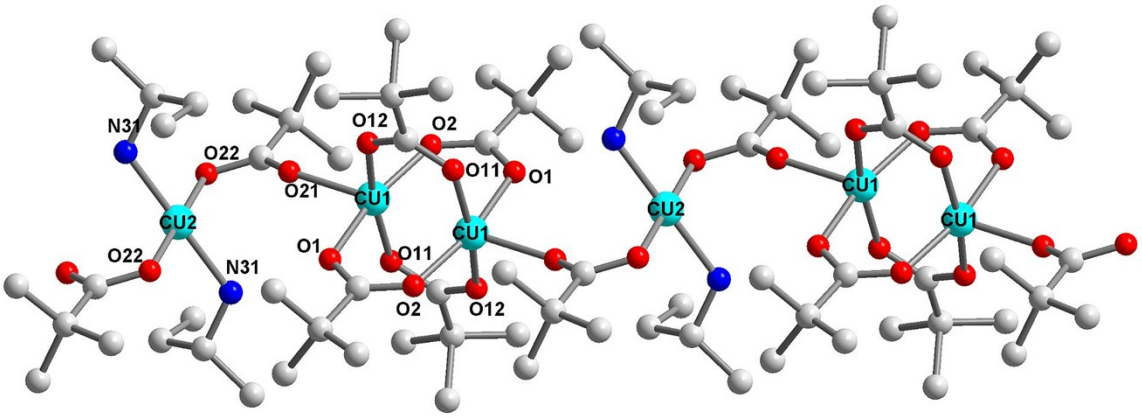

Figure S1 Chain topology in $[Cu_3(^sBuNH_2)_2(\mu\text{-}O_2C^tBu)_6]_n$ (**2a**) shows alternately arranged paddlewheel and mononuclear motifs.

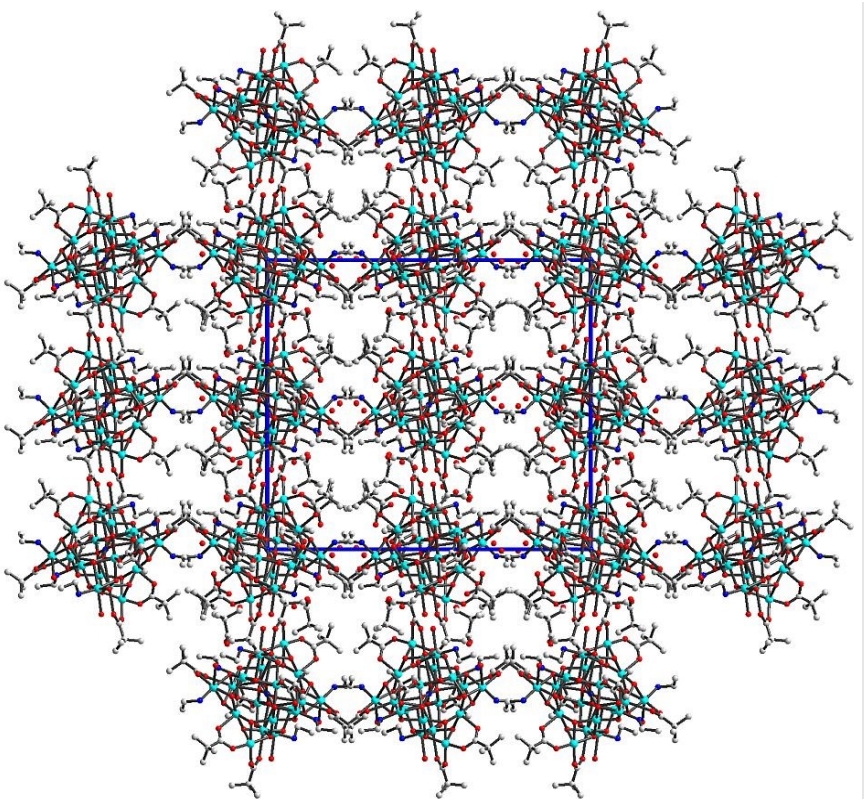

Figure S 2 Packing diagram of $[Cu_{20}(EtNH_2)_6(\mu_3\text{-}OH)_{24}(OH)(H_2O)_5(NO_3)(\mu\text{-}O_2C^tBu)_8](^tBuCO_2)_6\cdot 13H_2O$ **(4a)** viewed along a axis. For the clarity of the picture hydrogen atoms are omitted.

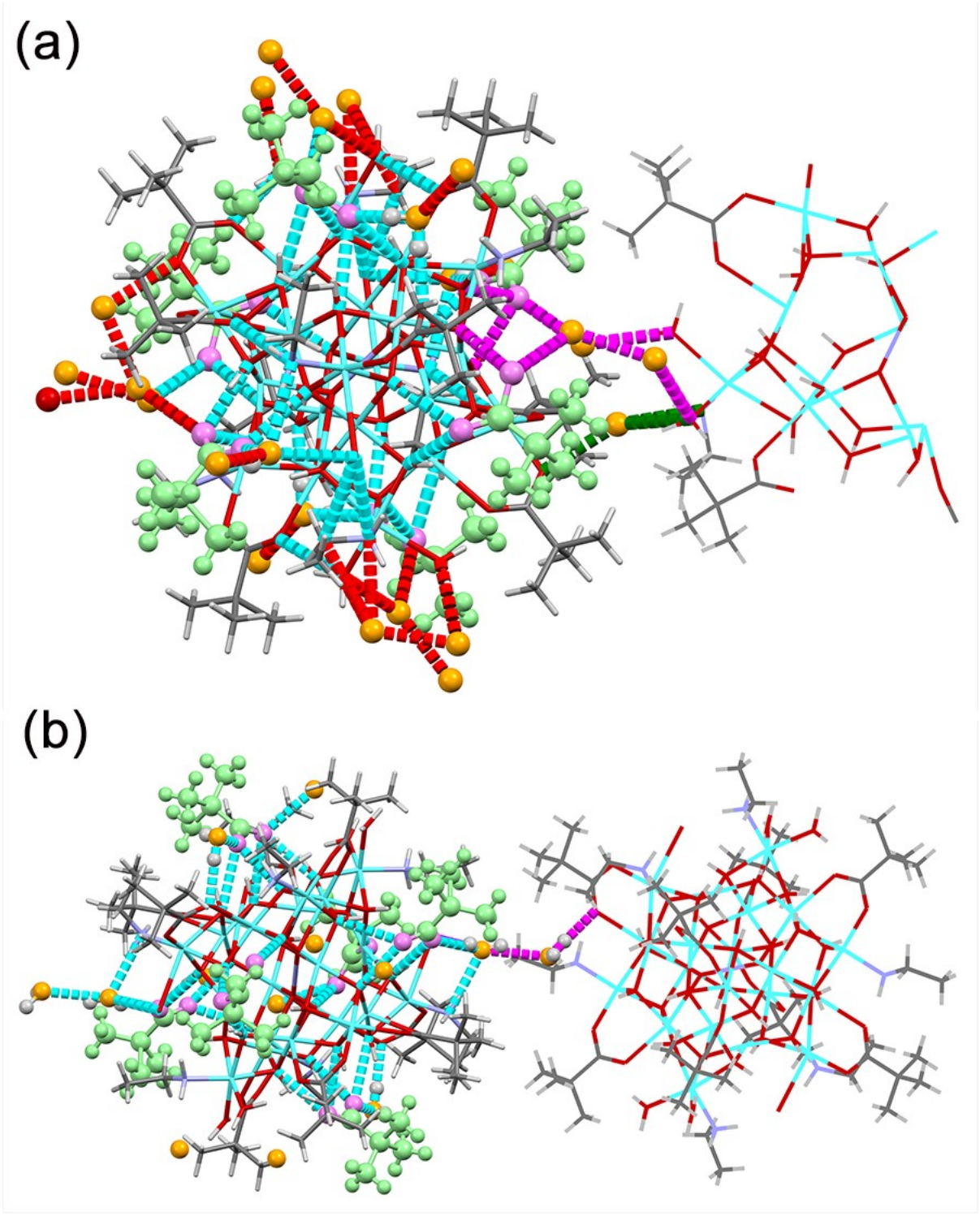

Figure S 3 The solvation sphere around the cluster (a) and hydrogen bonds in the crystal network (b). The selected hydrogen bond pathways between clusters are marked in green (for cluster…solvation sphere…cluster pattern) and in magenta (for cluster…solvation sphere…solvation sphere…cluster pattern).

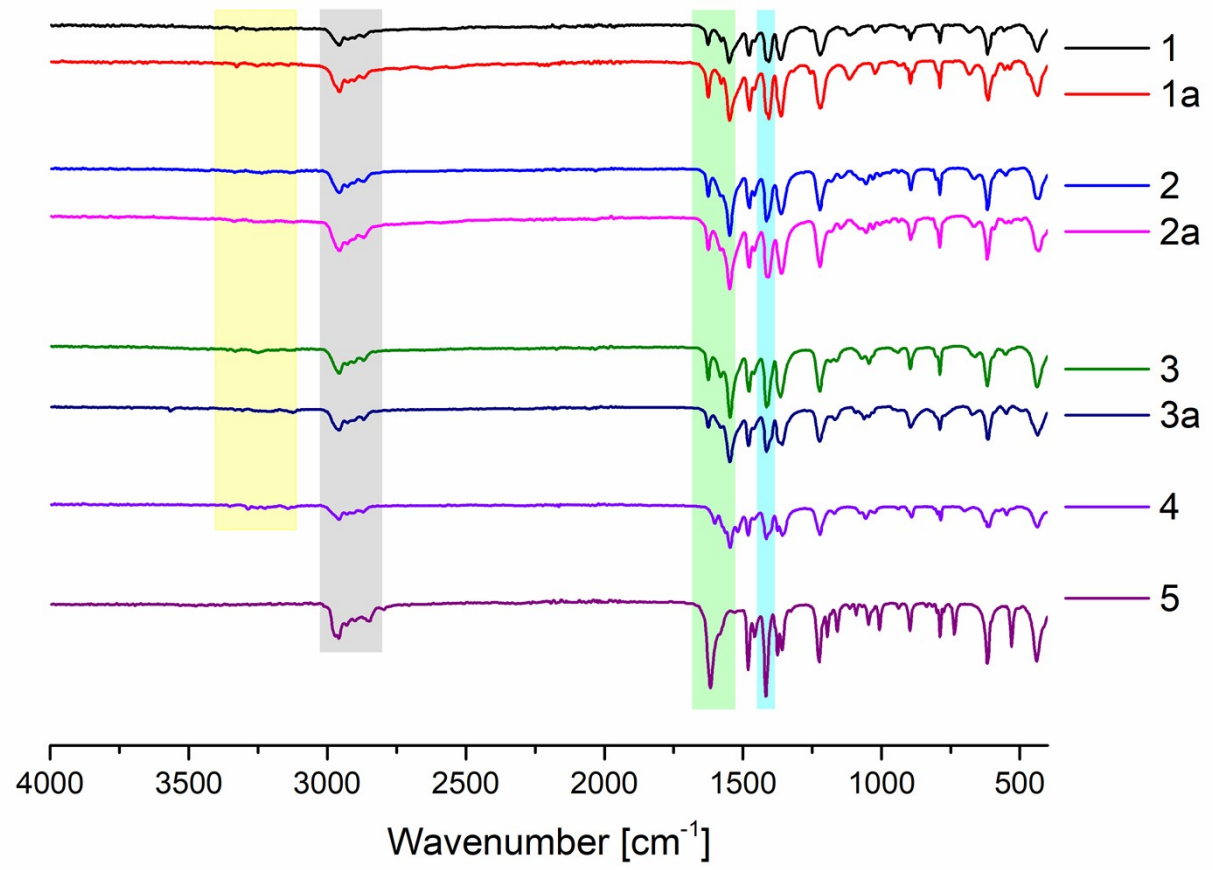

Figure S 4 ATR-IR spectrum for the compounds in the general formulas: $[Cu_2(RNH_2)_2(\mu\text{-}O_2C^tBu)_4]_n$ (**1−5**) and single crystals formed during crystallization **(1a−3a)**. The coloured bands highlight the ranges of the particular vibrational modes: (νNH_2) (yellow), ($\nu_{as}COO$) (green), (ν_sCOO) (blue), (νCH_3) (grey).

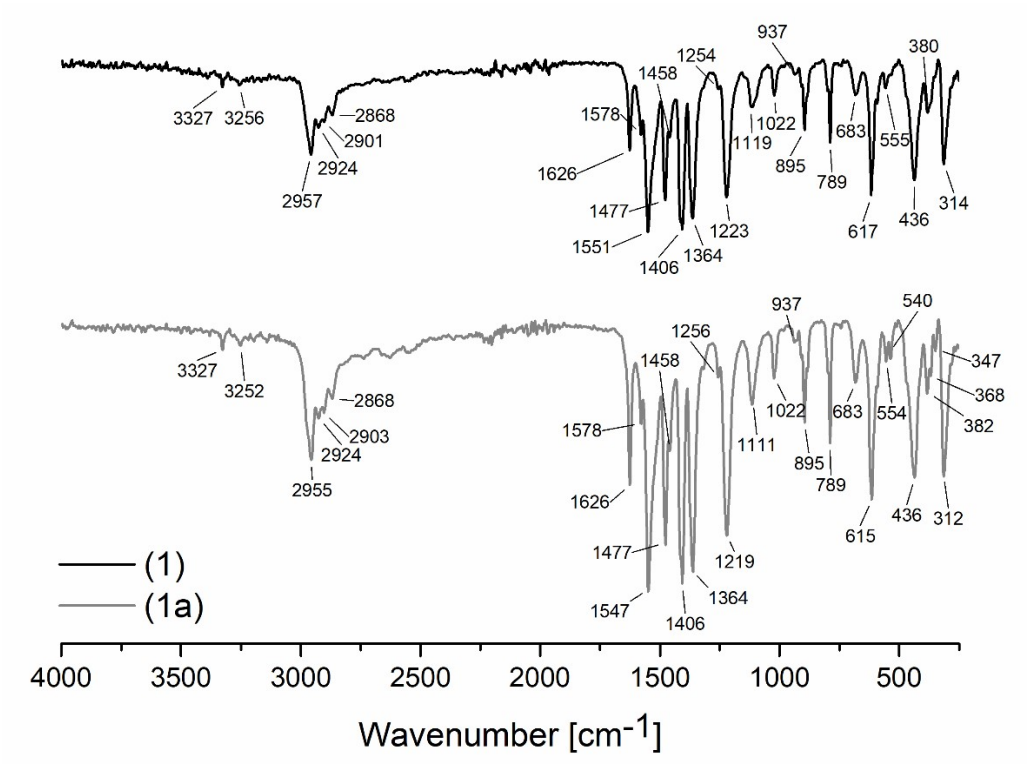

Figure S5 ATR-IR spectrum for the compound $[Cu_2(^tBuNH_2)_2(\mu\text{-}O_2C^tBu)_4]_n$ **(1)** (black) and $[Cu_3(^tBuNH_2)_2(\mu\text{-}O_2C^tBu)_6]_n$ (**1a**) (grey).

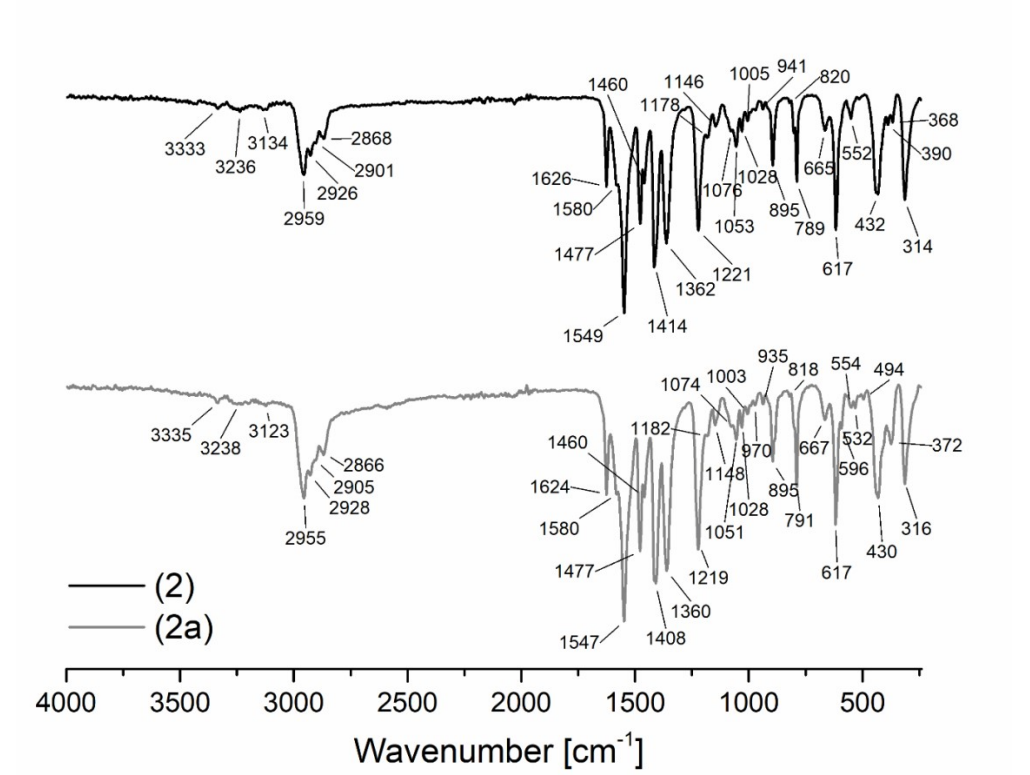

Figure S6 ATR-IR spectrum for the compound $[Cu_2(^sBuNH_2)_2(\mu\text{-}O_2C^tBu)_4]_n$ (**2**) (black) and $[Cu_3(^sBuNH_2)_2(\mu\text{-}O_2C^tBu)_6]_n$ (**2a**) (grey).

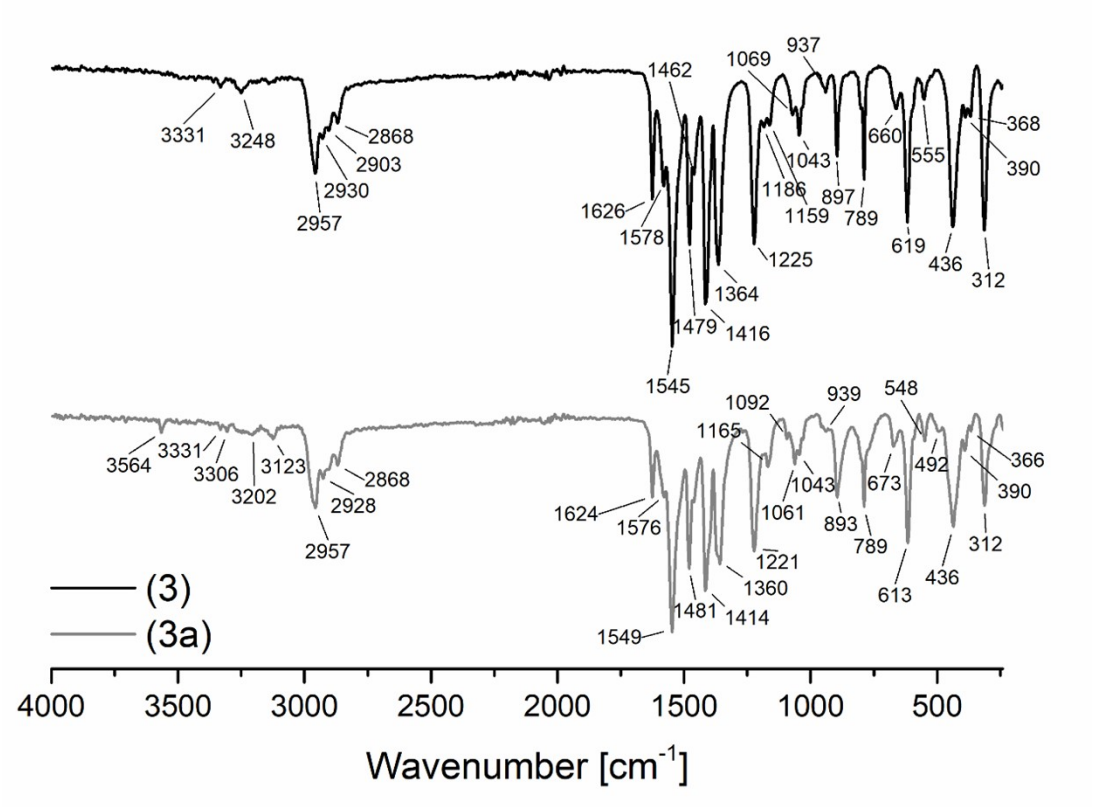

Figure S7 ATR-IR spectrum for the compound $[Cu_2(^iPrNH_2)_2(\mu\text{-}O_2C^tBu)_4]_n$ (**3**) (black) and $[Cu_3(^iPrNH_2)_2(\mu_3\text{-}OH)_2(\mu\text{-}O_2C^tBu)_4]_n$ (**3a**) (grey).

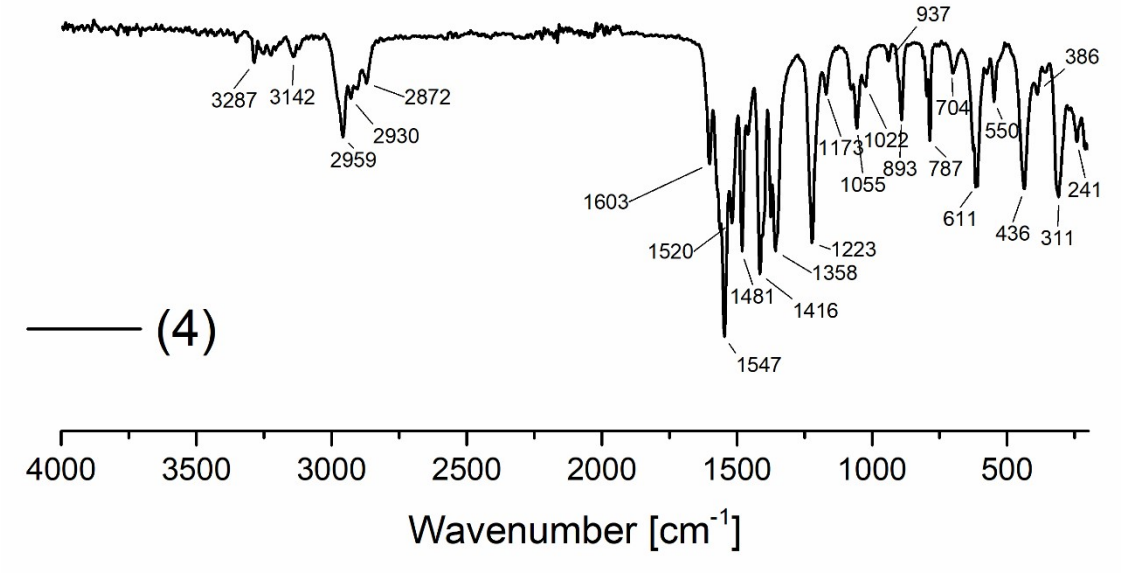

Figure S8 ATR-IR spectrum for the compound $[Cu_2(EtNH_2)_2(\mu\text{-}O_2C^tBu)_4]_n$ (**4**).

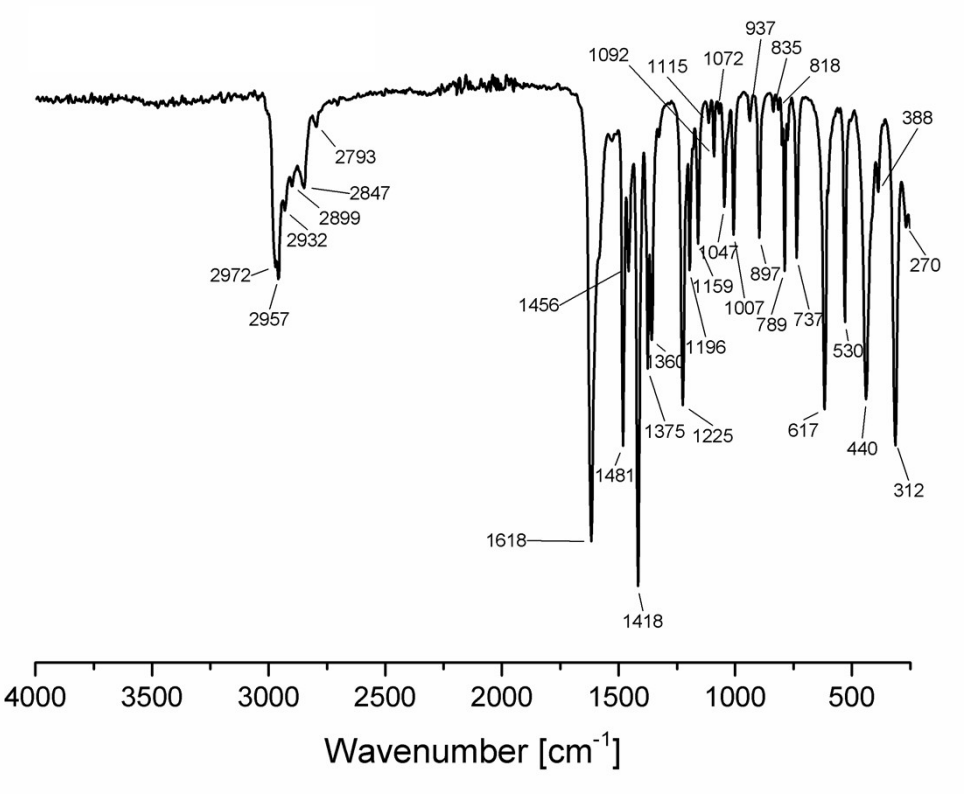

Figure S9 ATR-IR spectrum for the compound $[Cu_2(Et_3N)_2(\mu\text{-}O_2C^tBu)_4]$ (**5**).

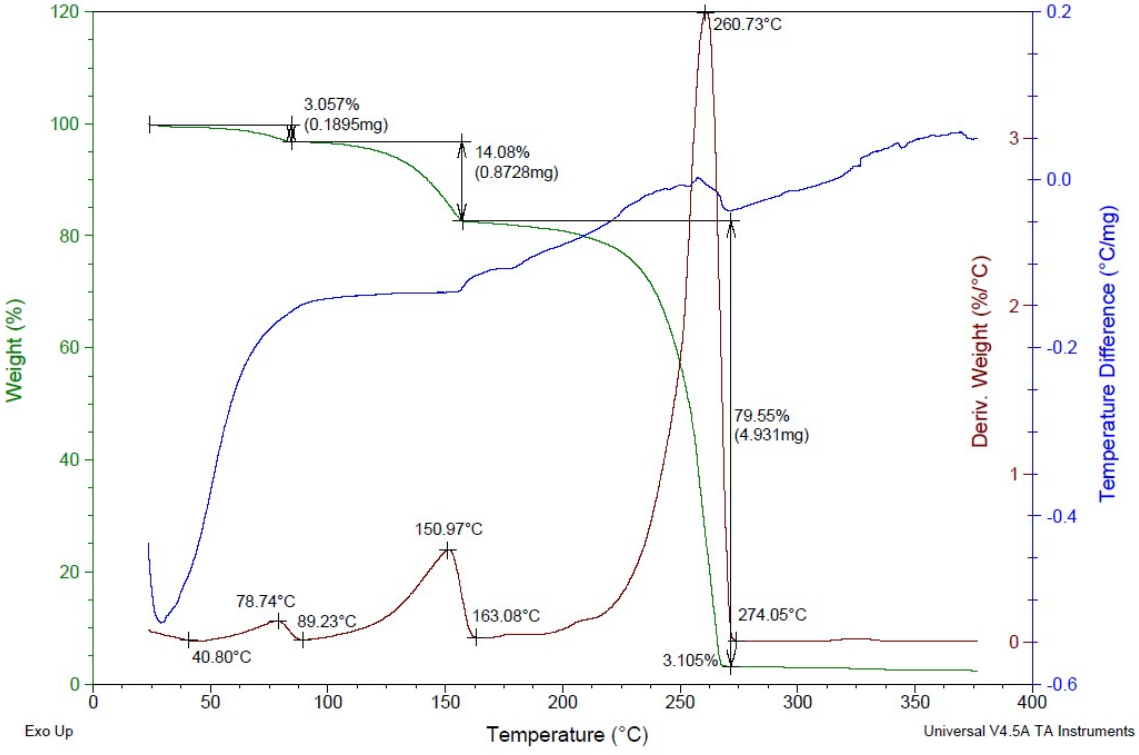

Figure S10 Thermal decomposition of $[Cu_2(^tBuNH_2)_2(\mu\text{-}O_2C^tBu)_4]_n$ (**1**) (TG, DTG, DTA curves).

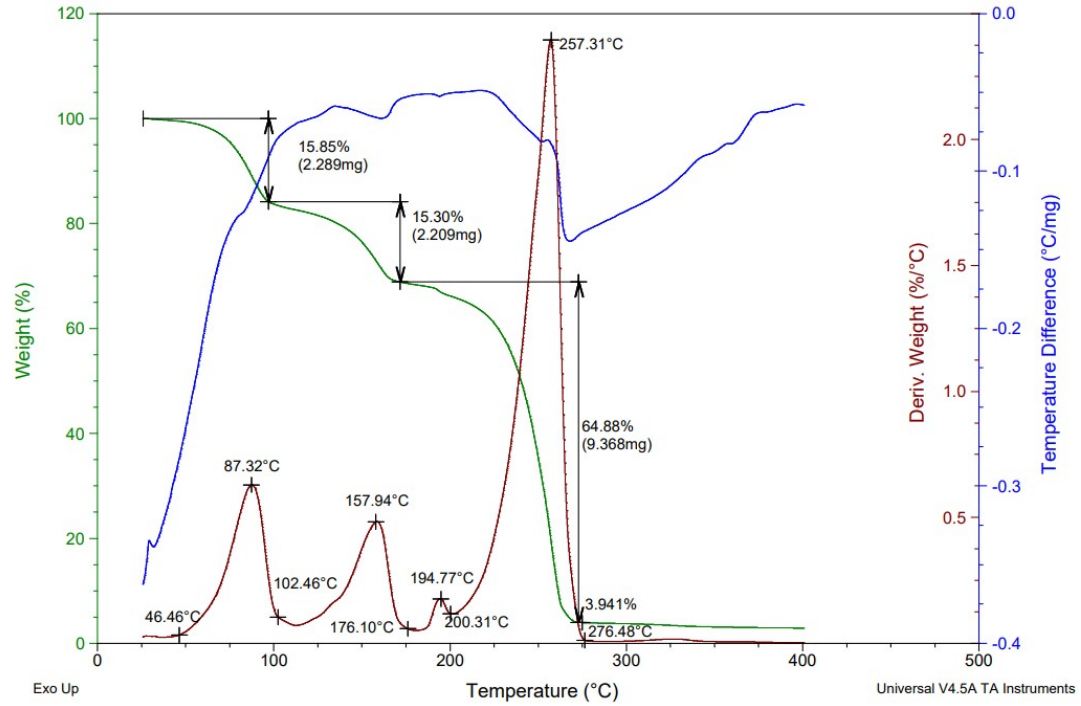

Figure S11 Thermal decomposition of $[Cu_2(^sBuNH_2)_2(\mu\text{-}O_2C^tBu)_4]_n$ (**2**) (TG, DTG, DTA curves).

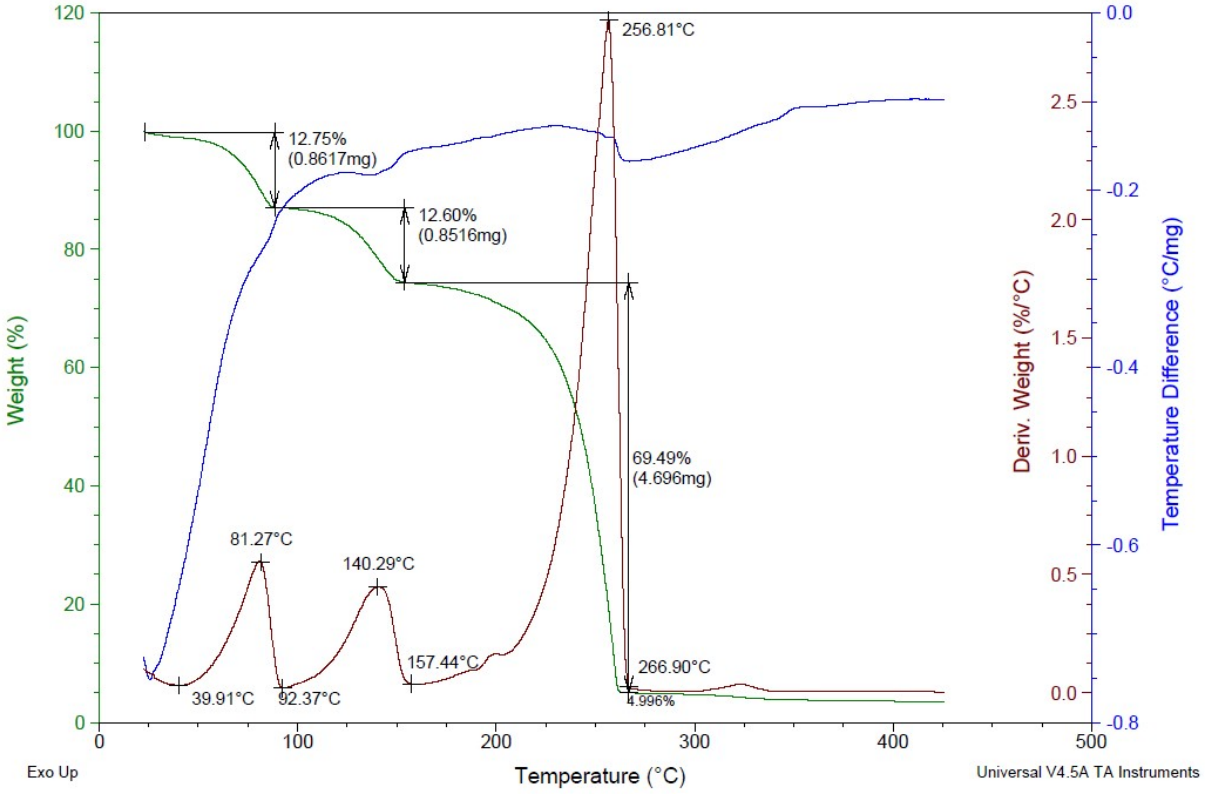

Figure S12 Thermal decomposition of $[Cu_2(^iPrNH_2)_2(\mu\text{-}O_2C^tBu)_4]_n$ (**3**) (TG, DTG, DTA curves).

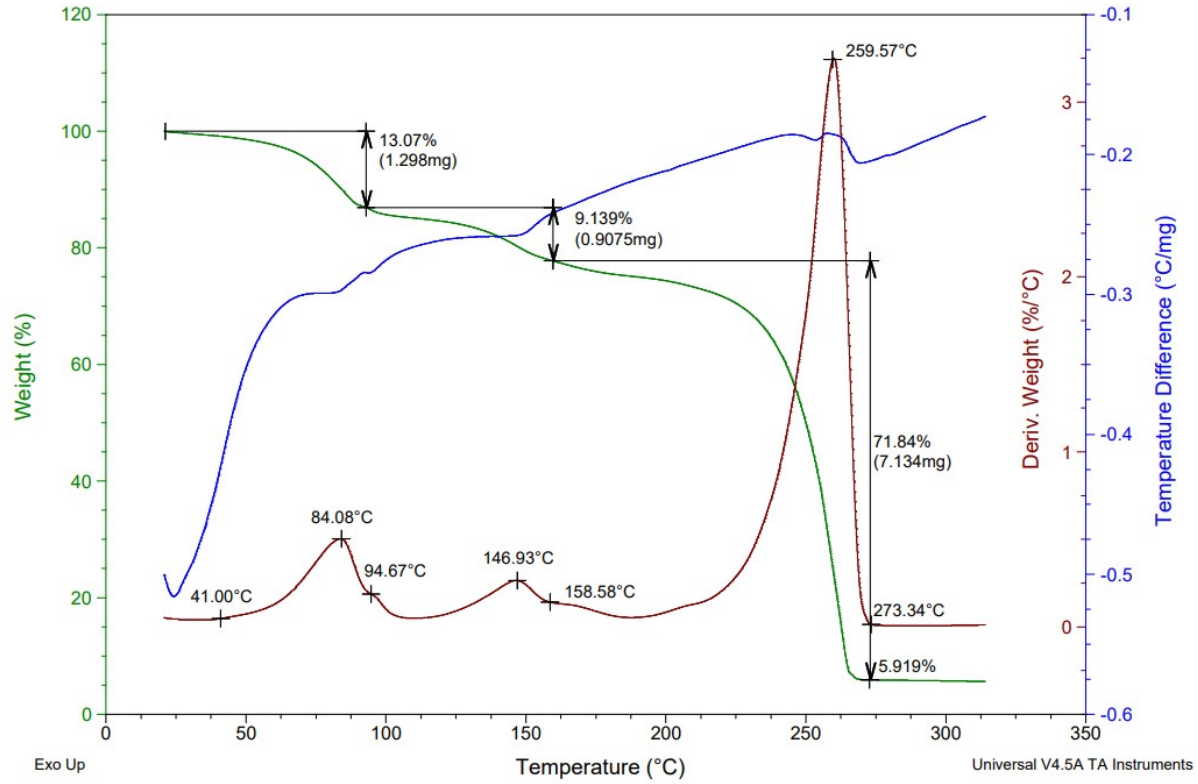

Figure S13 Thermal decomposition of $[Cu_2(EtNH_2)_2(\mu\text{-}O_2C^tBu)_4]_n$ (**4**) (TG, DTG, DTA curves).

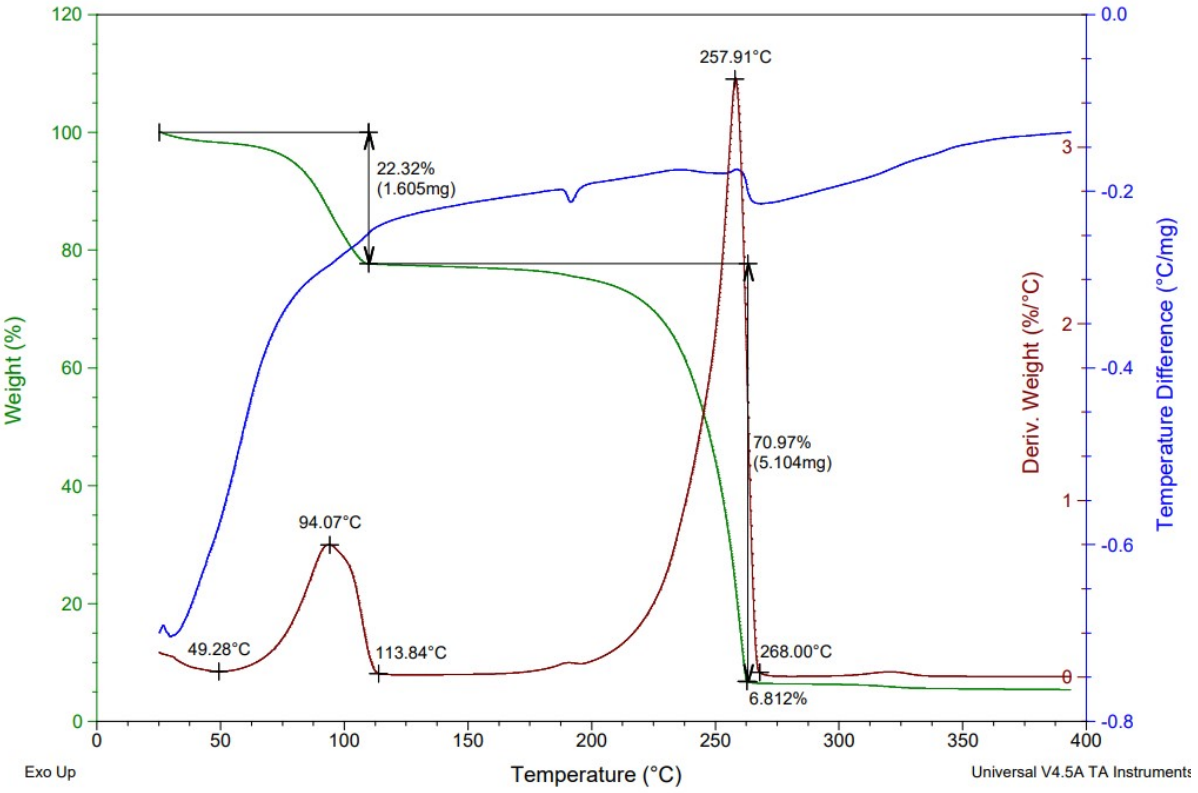

Figure S14 Thermal decomposition of $[Cu_2(Et_3N)_2(\mu\text{-}O_2C^tBu)_4]$ (**5**) (TG, DTG, DTA curves).

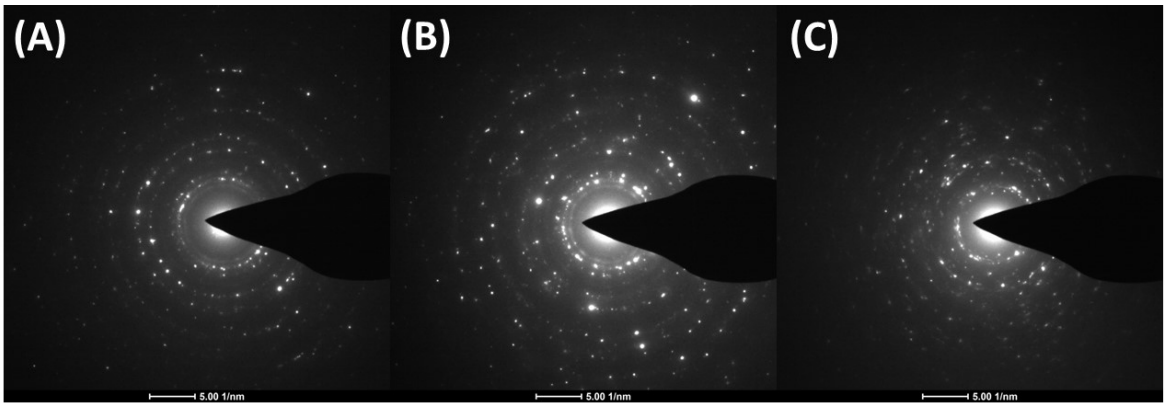

Figure S15 Transmission electron microscope (TEM) diffraction pattern for the TGA final residue: **(A)** $[Cu_2(^sBuNH_2)_2(\mu\text{-}O_2C^tBu)_4]_n$ **(2)**, **(B)** $[Cu_2(^iPrNH_2)_2(\mu\text{-}O_2C^tBu)_4]_n$ **(3),** and **(C)** $[Cu_2(Et_3N)_2(\mu\text{-}O_2C^tBu)_4]$ **(5)**.

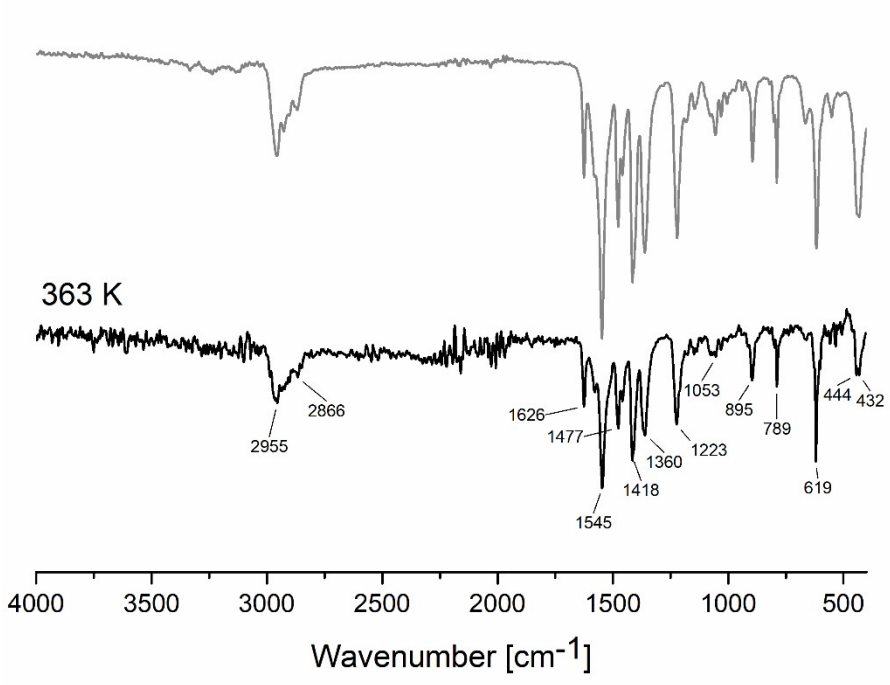

Figure S16 Infrared spectra for the compound $[Cu_2(^sBuNH_2)_2(\mu\text{-}O_2C^tBu)_4]_n$ (**2**) before (grey) and after sublimation (black) at 363 K ($p = 10^{-2}$ mbar).

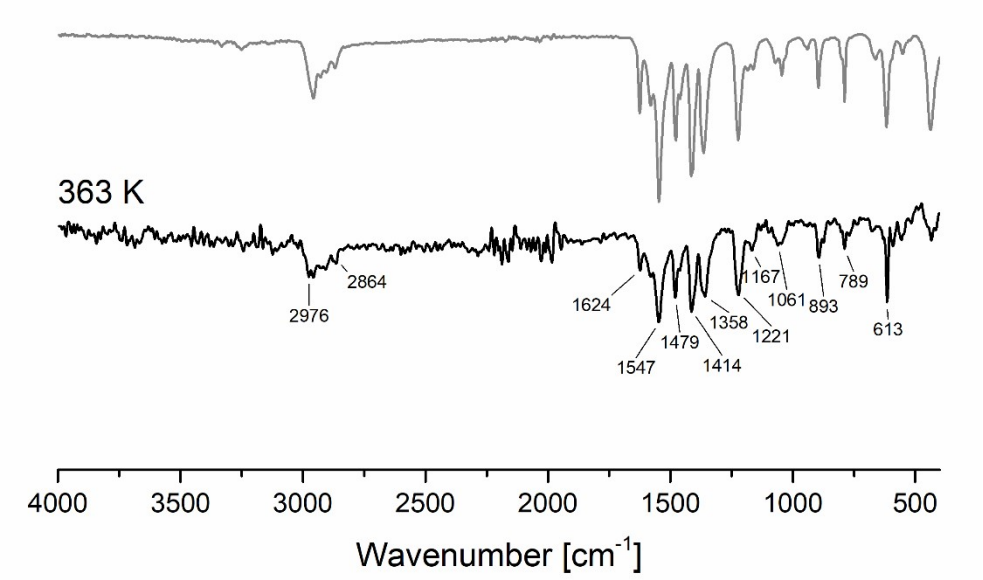

Figure S17 Infrared spectra for the compound $[Cu_2(^iPrNH_2)_2(\mu\text{-}O_2C^tBu)_4]_n$ (**3**) before (grey) and after sublimation (black) at 363 K ($p = 10^{-2}$ mbar).

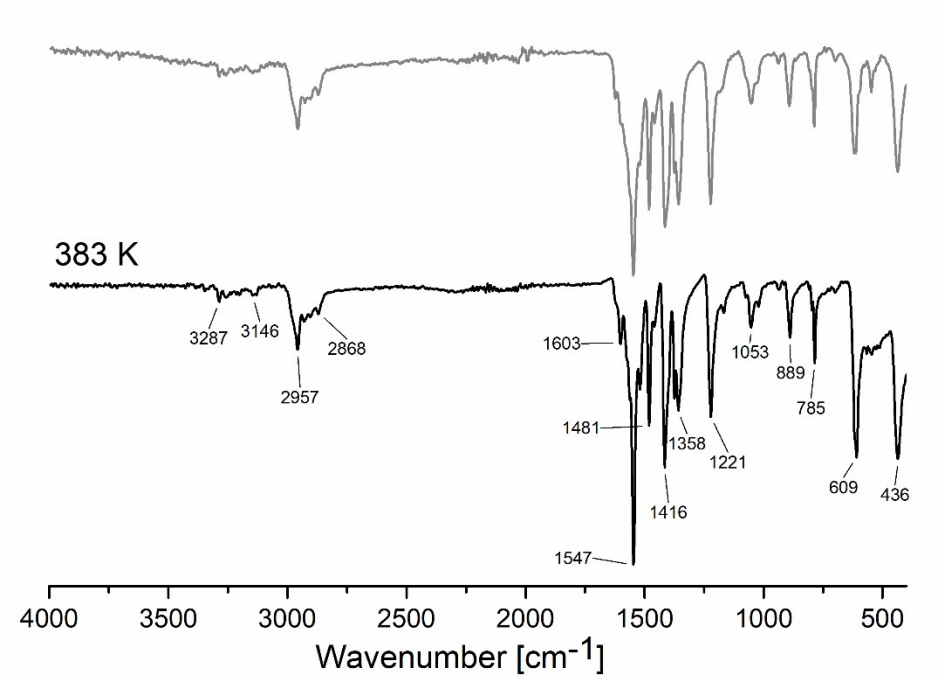

Figure S18 Infrared spectra for the compound $[Cu_2(EtNH_2)_2(\mu\text{-}O_2C^tBu)_4]_n$ (**4**) before (grey) and after sublimation (black) at 383 K ($p = 10^{-2}$ mbar).

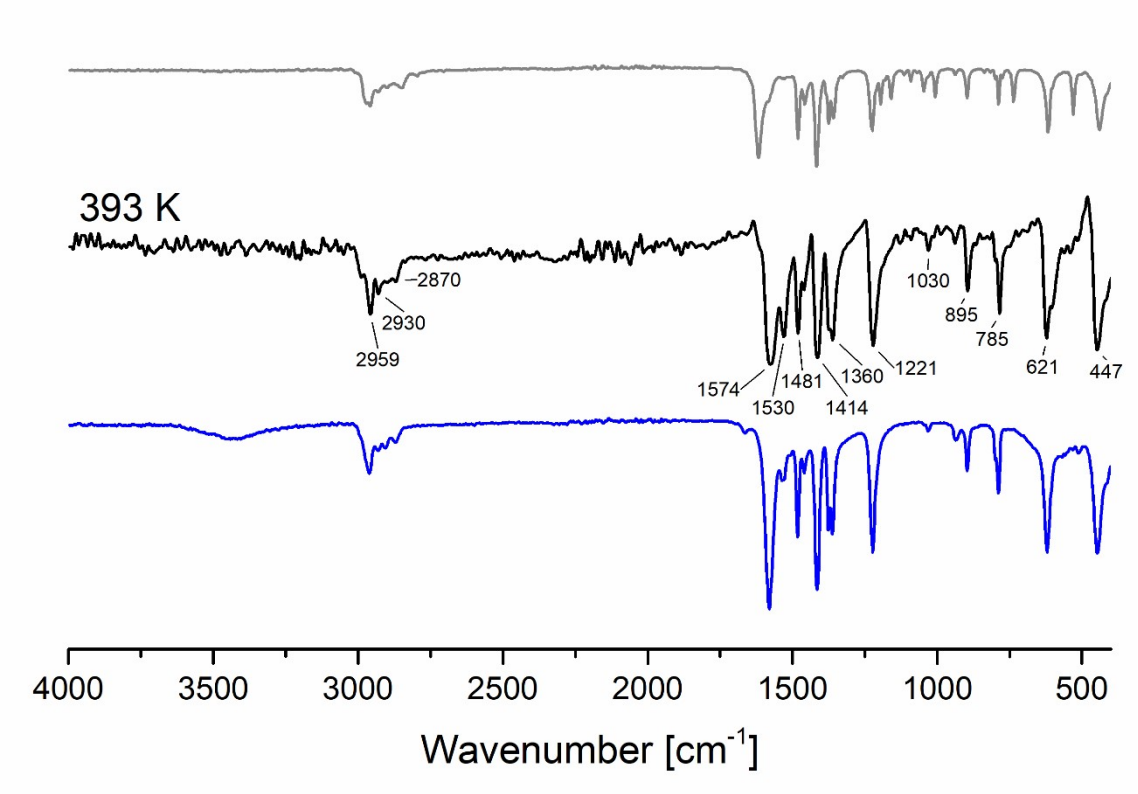

Figure S19 Infrared spectra for the compound $[Cu_2(Et_3N)_2(\mu\text{-}O_2C^tBu)_4]$ (**5**) before (grey) and after sublimation attempt (black) at 393 K ($p = 10^{-2}$ mbar), $[Cu_2(\mu\text{-}O_2C^tBu)_4]_n$ **(0)** (blue).

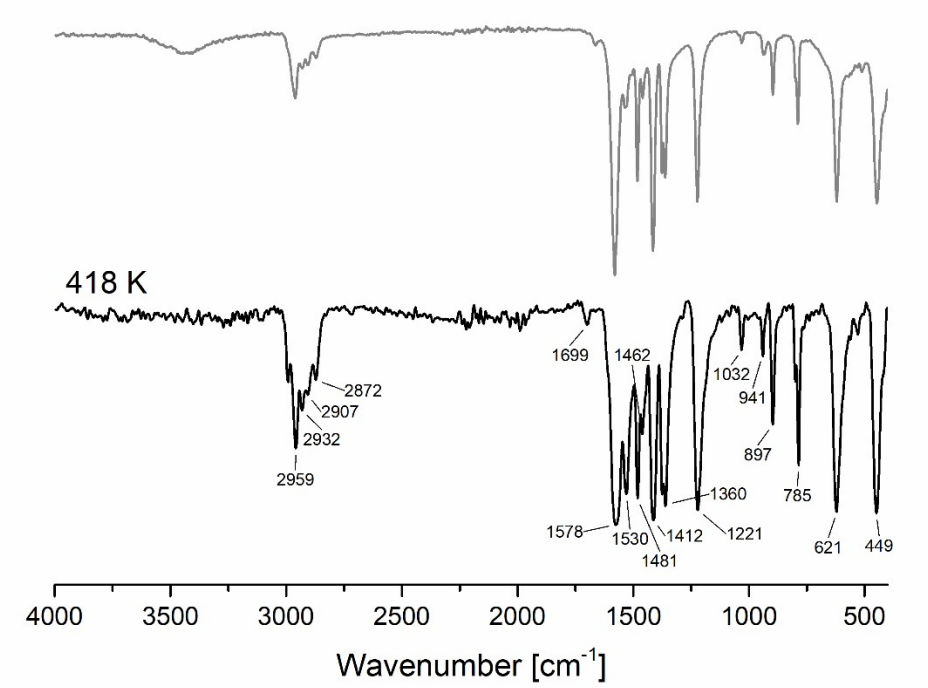

Figure S20 Infrared spectra for the compound $[Cu_2(\mu\text{-}O_2C^tBu)_4]_n$ **(0)** before (grey) and after sublimation (black) at 418 K ($p = 10^{-2}$ mbar).

Table S6 Mass spectrometry with electron ionization (EI MS) results for the complex $[Cu_2(^tBuNH_2)_2(\mu\text{-}O_2C^tBu)_4]$ (**1**).

Fragments	*m/z*	Relative Intensity (RI) [%]				
		350 K	**370 K**	**417 K**	**487 K**	**525 K**
$[C_2H_2N]^+/[CH_2{=}C{=}CH_2]^{+\cdot}$	40	6	11	45	50	40
$[C_2H_3N]^+/[CH_2{=}CH{-}CH_2]^{+\cdot}$	41	1	21	8	10	–
$[C_2H_4N]^+/[CH_2CO]^+$	42	26	35	92	94	88
$[CO_2]^{+\cdot}$	44	3	1	2	8	–
$[C_2H_7N]^+/[COOH]^{+\cdot}$	45	1	–	33	100	25
$[(CH_3)_2C{=}CH_2]^{+\cdot}$	56	2	2	12	21	–
$[^tBu]^+$	57	4	1	29	24	–
$[C_3H_8N]^+/[C_4H_{10}]^{+\cdot}$	58	48	100	100	99	100
$[C_3H_9N]^{+\cdot}$	59	100	26	5	5	8
$[Cu]^+$	63	1	11	1	–	–
$[C_3H_7CO_2]^+$	87	1	–	5	5	–
$[CuCO_2]^+$	107	1	6	–	–	–
$[Cu_2(^tBu)]^+$	183	3	2	8	–	–
$[Cu_2(O_2C^tBu)]^+$	227	14	27	36	–	–
$[Cu_2(O_2C^tBu)_2]^{+\cdot}$	328	12	25	23	–	–
$[Cu_3(O_2C^tBu)_2]^+$	393	–	6	–	–	–
$[Cu_3(O_2C^tBu)_5]^+$	696	1	4	–	–	–

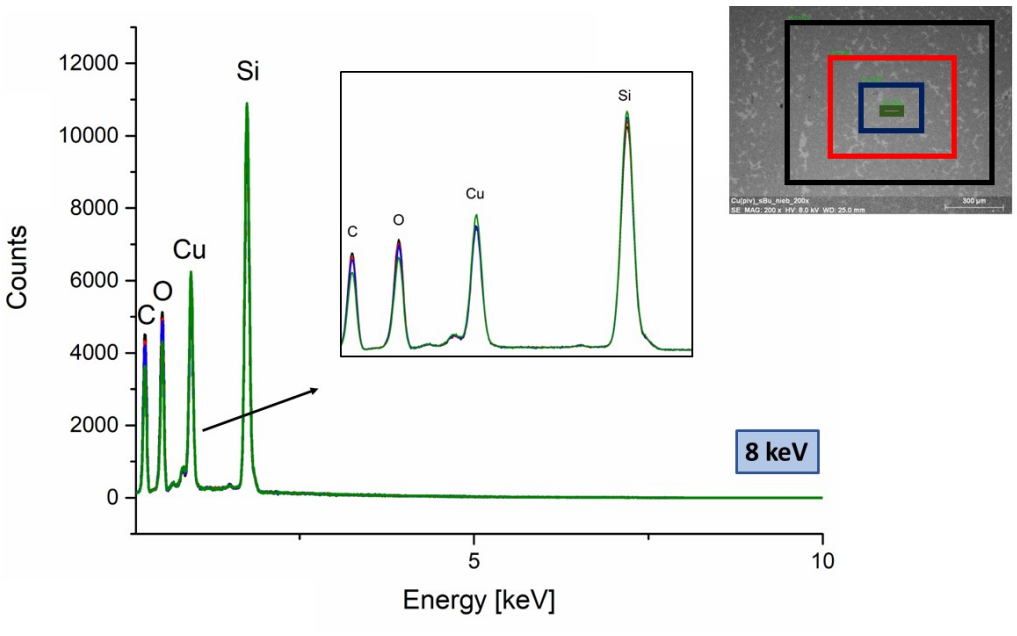

Figure S21 Examined scan areas' EDX spectra (8 keV) for $[Cu_2(^sBuNH_2)_2(\mu\text{-}O_2C^tBu)_4]_n$ (**2**) layer on a silicon wafer.

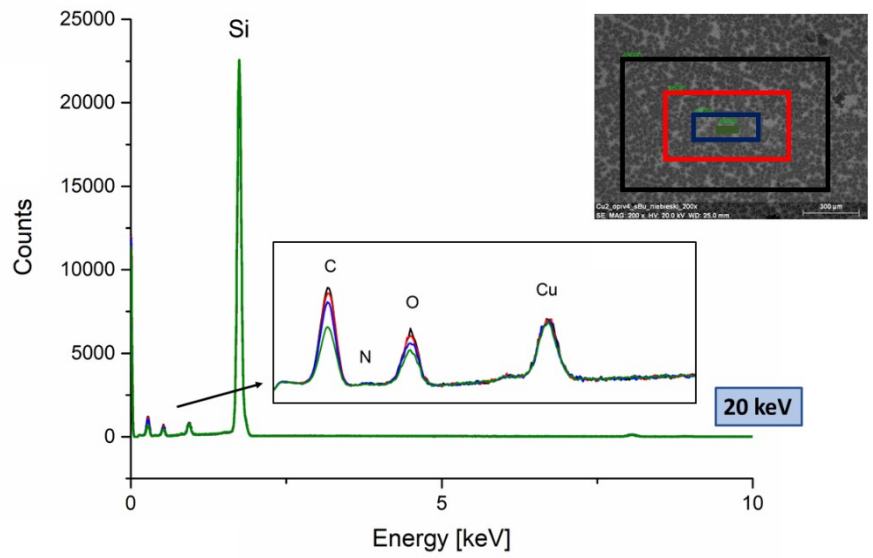

Figure S22 Examined scan areas' EDX spectra (20 keV) for $[Cu_2(^sBuNH_2)_2(\mu\text{-}O_2C^tBu)_4]_n$ (**2**) layer on a silicon wafer.

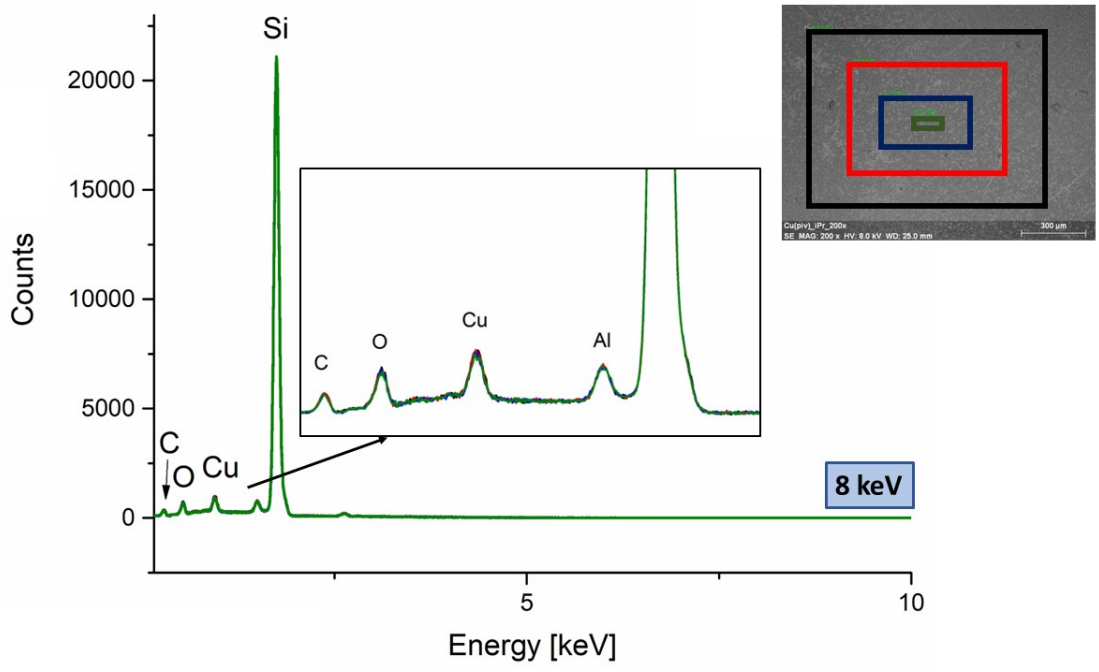

Figure S23 Examined scan areas' EDX spectra (8 keV) for $[Cu_2(^iPrNH_2)_2(\mu\text{-}O_2C^tBu)_4]_n$ (**3**) layer on a silicon wafer.

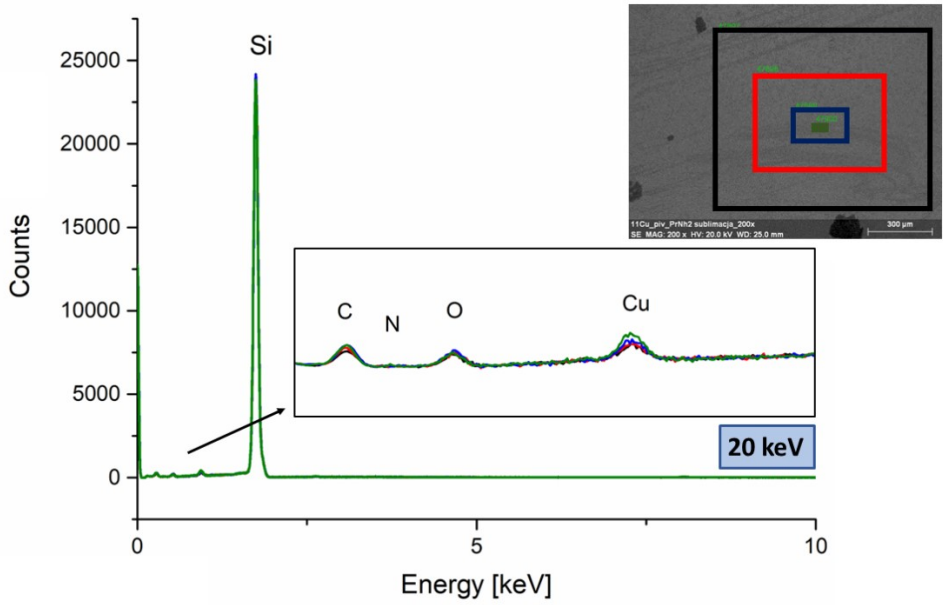

Figure S24 Examined scan areas' EDX spectra (20 keV) for $[Cu_2(^iPrNH_2)_2(\mu\text{-}O_2C^tBu)_4]_n$ (**3**) layer on a silicon wafer.

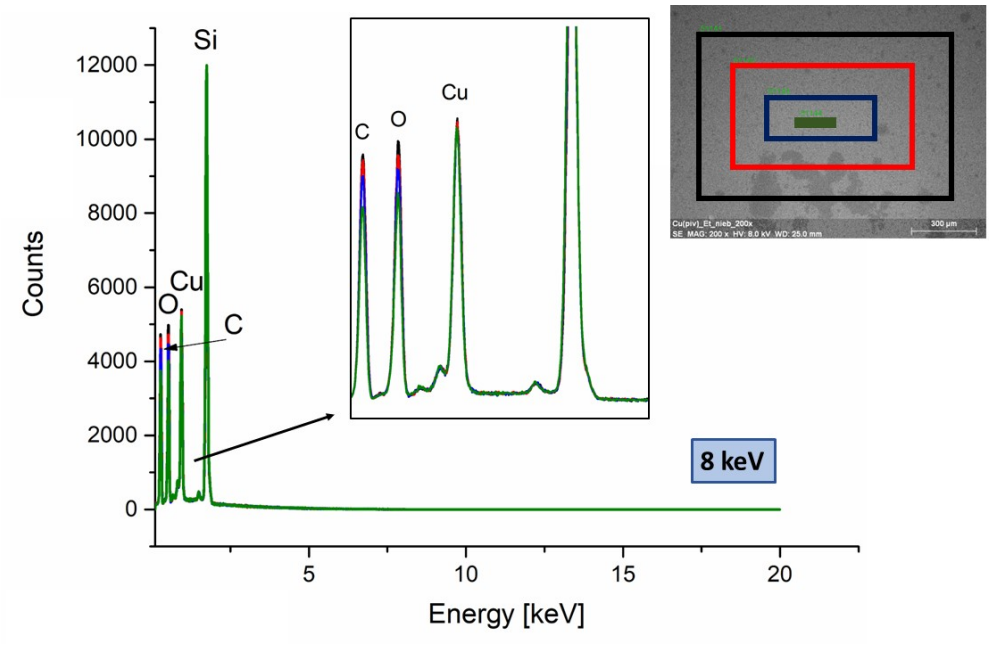

Figure S25 Examined scan areas' EDX spectra (8 keV) for $[Cu_2(EtNH_2)_2(\mu\text{-}O_2C^tBu)_4]_n$ (**4**) layer on a silicon wafer.

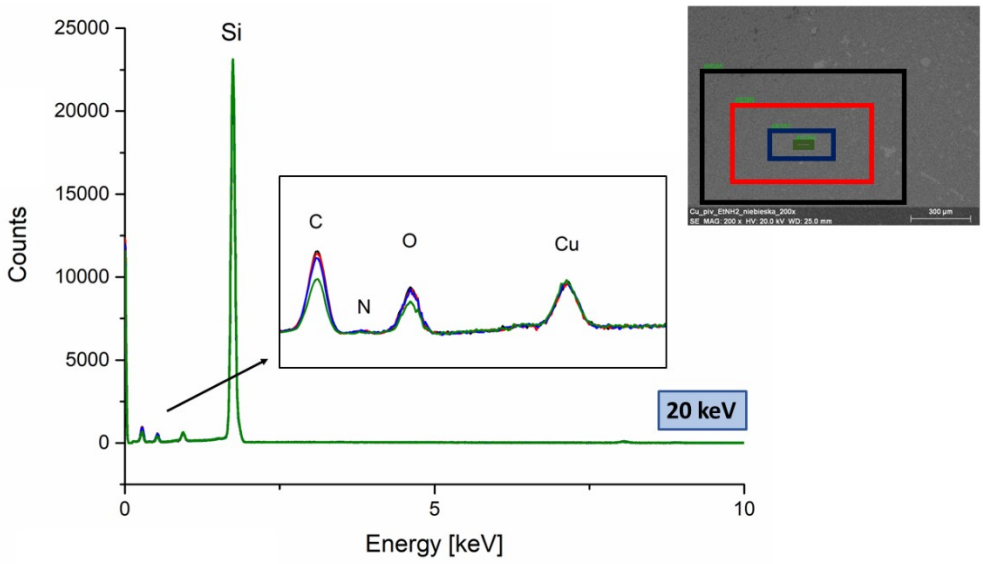

Figure S26 Examined scan areas' EDX spectra (20 keV) for $[Cu_2(EtNH_2)_2(\mu\text{-}O_2C^tBu)_4]_n$ (**4**) layer on a silicon wafer.

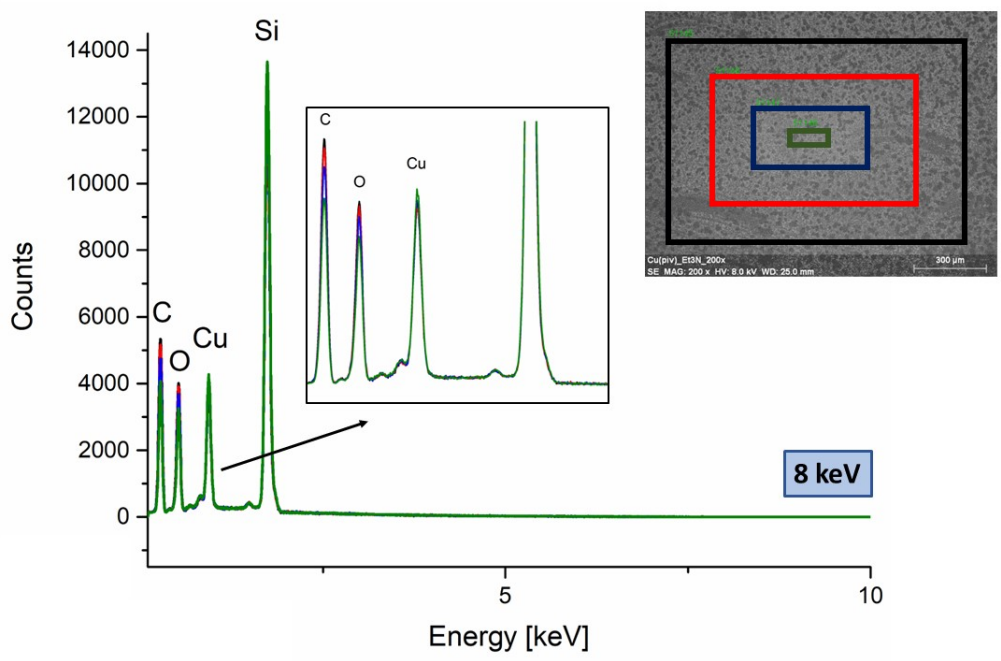

Figure S27 Examined scan areas' EDX spectra (8 keV) for $[Cu_2(Et_3N)_2(\mu\text{-}O_2C^tBu)_4]$ (**5**) layer on a silicon wafer.

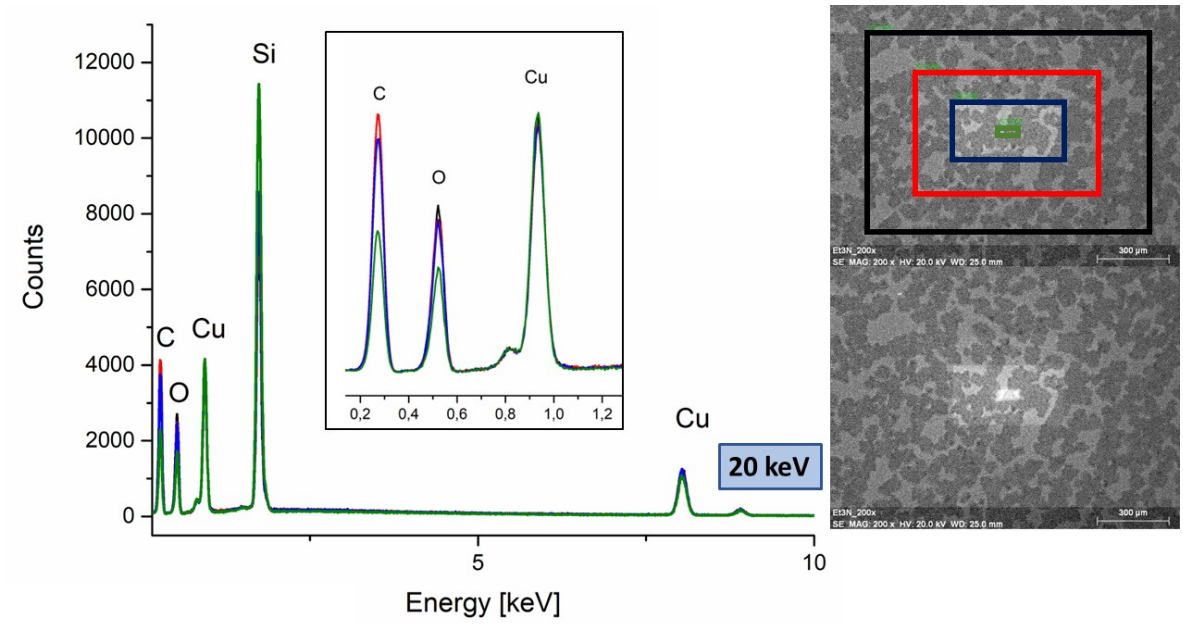

Figure S28 Examined scan areas' EDX spectra (20 keV) for $[Cu_2(Et_3N)_2(\mu\text{-}O_2C^tBu)_4]$ (**5**) layer on a silicon wafer.

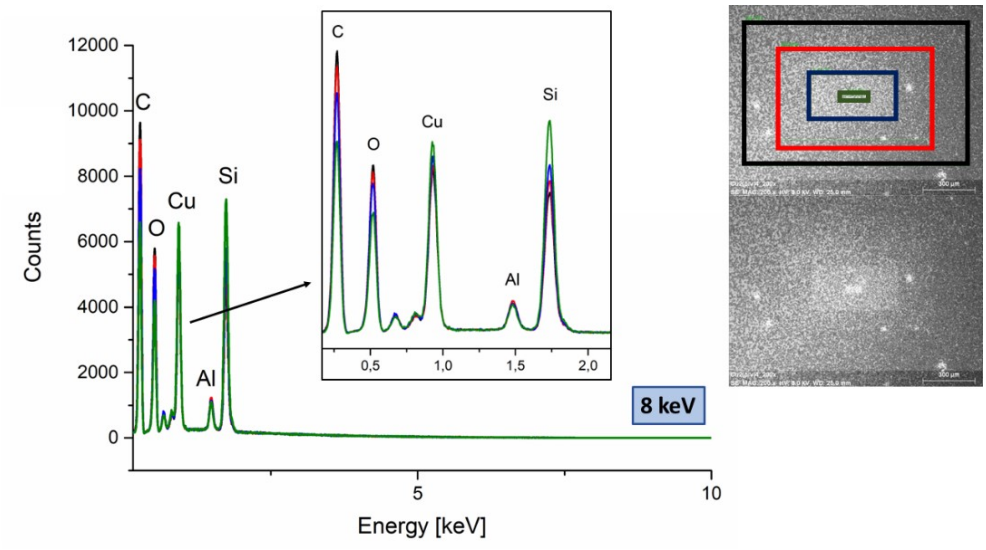

Figure S29 Examined scan areas' EDX spectra (8 keV) for $[Cu_2(\mu\text{-}O_2C^tBu)_4]_n$ **(0)** layer on a silicon wafer.

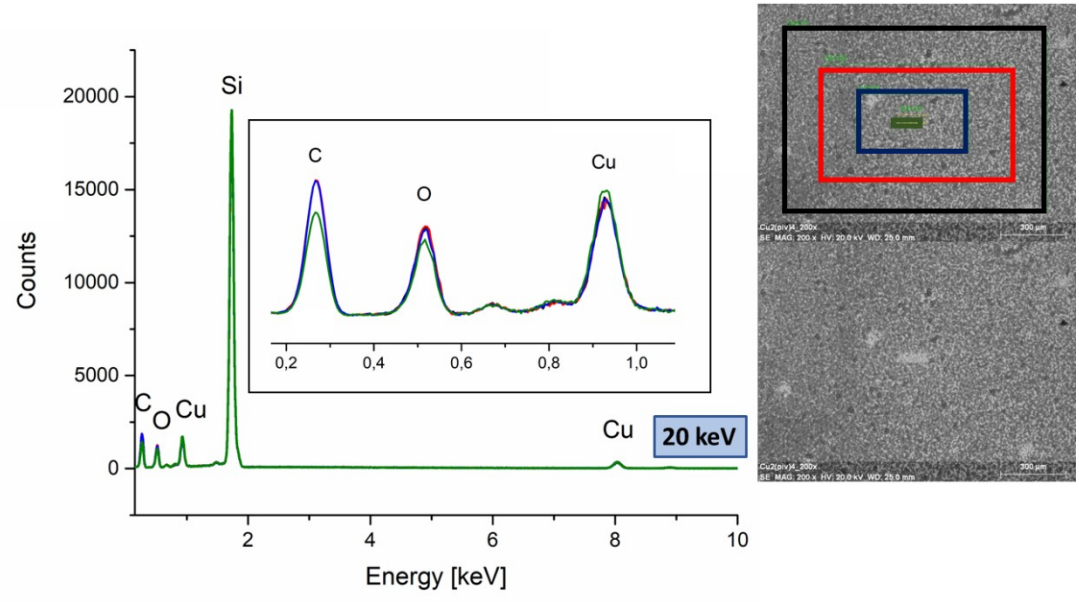

Figure S30 Examined scan areas' EDX spectra (20 keV) for $[Cu_2(\mu\text{-}O_2C^tBu)_2]_n$ **(0)** layer on a silicon wafer.

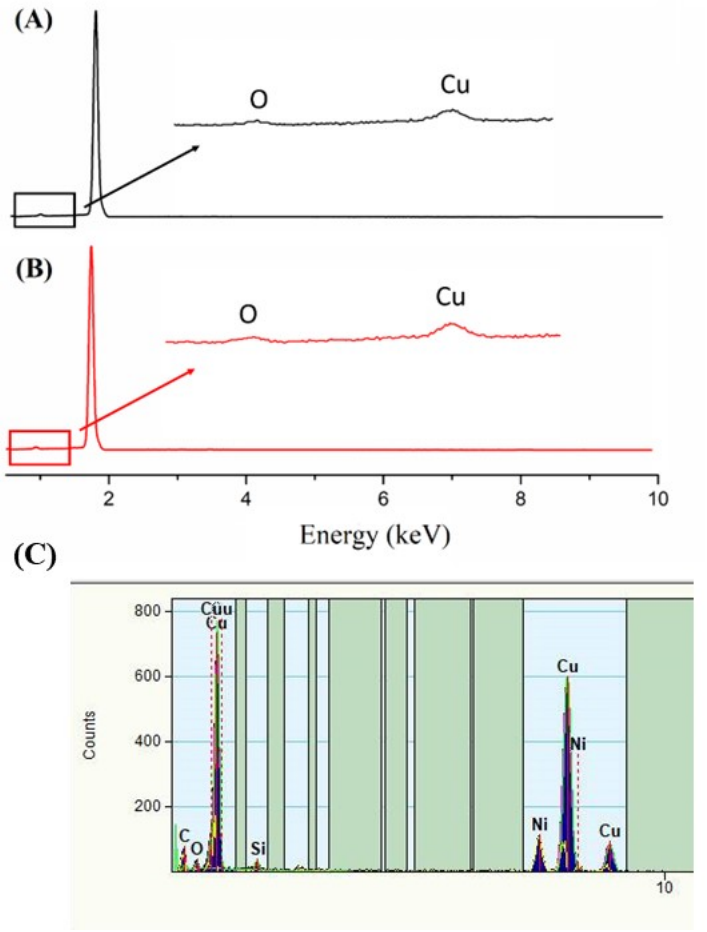

Figure S31 Composition analysis of the obtained materials using $[Cu_2(^tBuNH_2)_2(\mu\text{-}O_2C^tBu)_4]_n$ (**1**), (**A**) for deposit obtained on the second substrate, (**B**) for deposit obtained on the fourth substrate, (**C**) EDX spectra from TEM obtained on the fourth substrate.

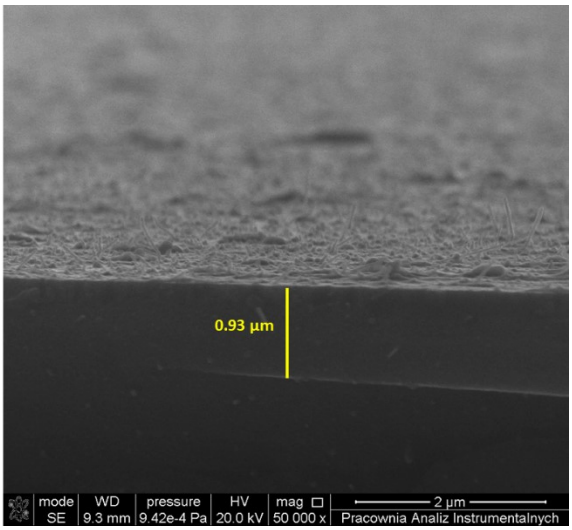

Figure S 32 SEM image to show the thickness of the copper layer obtained materials using $[Cu_2(^tBuNH_2)_2(\mu\text{-}O_2C^tBu)_4]_n$ (**1**) for deposit obtained on the second substrate.